Comparisons of Two Different Analytical Methodologies for the Characterization of Sub-Visible Particles in Therapeutic Protein Formulations

by

Dipl.-Chem. (FH) Tobias Frommknecht

submitted to the graduate degree program in Pharmaceutical Chemistry and the Graduate Faculty of the University of Kansas in partial fulfillment of the requirements for the degree of Master of Sciences.

_____

Chairperson, Professor David B. Volkin, Ph.D.

_____

PD Dr. Hanns-Christian Mahler

_____

Professor Susan M. Lunte, Ph.D.

Date Defended: December 12, 2011

The Thesis Committee for Tobias Frommknecht

certifies that this is the approved version of the following thesis:

Comparisons of Two Different Analytical Methodologies for the Characterization of Sub-Visible Particles in Therapeutic Protein Formulations

_____

Chairperson, Professor David B. Volkin, Ph.D.

_____

PD Dr. Hanns-Christian Mahler

_____

Professor Susan M. Lunte, Ph.D.

Date approved: December 12, 2011

Abstract

The US and EU pharmacopeias require sub-visible particle (SbVP) testing of parenteral drug products by either light obscuration (LO) or light microscopy.[1-3] According to the USP/EP, the LO method requires the use of four measurements consuming a total volume of 25 ml per sample.[1-3] This large sample volume makes the compendia test not only cost-intensive for biopharmaceutics, but in certain cases impractical, especially in early stage development when clinical supplies are often limited. The first part of this work therefore presents a set of experimental data for evaluation of a small scale, lower volume LO method (1.2 ml per sample). Limitations for detecting various translucent particles such as glass splinters, silicone oil droplets and non-soluble protein aggregates have been considered for both of these LO methods. In addition, a relatively new technology – Micro Flow Digital Imaging (MDI) – has been introduced, which may be a viable add-on to measure SbVP.[4-7] The purpose of the second phase of this research was to evaluate the advantages and limitations of MDI by directly comparing LO and MDI, and also by comparing two different MDI instruments (i.e., Micro Flow Imaging (MFI) and FlowCam), with regards to subvisible particle counts, size distribution and morphology parameter analysis.

As protein subvisible particles vary widely in shape and size, it is difficult to quantitatively describe the limitations of MDI and LO for actual samples of a protein therapeutic drug. Moreover, real-life protein formulations can differ in optical properties such as turbidity, color, refractive index which may potentially influence SbVP detection. During this work, MDI technologies have been improved for the use on a routine basis with protein samples (e.g., FlowCam counting ability was improved by adding a syringe pump for controlled flow, and MFI optical system was enhanced with the so called set-point 3). The effect of solution optical properties on SbVP particle sizing and counting was addressed subsequently using the latest MDI instrument and three different LO instruments. In addition,

translucent particles such as glass and irregular shaped particles in development as “false protein standard” (to mimic properties of real life proteinaceous particles) were evaluated in this work.

Acknowledgements

I gratefully thank Prof. David Volkin, PD Dr. Hanns-Christian Mahler, Dr. Michael Adler, Dr. Sylvia Kiese and Dr. Oliver Stauch for their help and support during this work, as well as Fluid Imaging Technologies and David Palmund for providing their “false protein standard”.

Table of Contents

Abbreviations

α	Alpha: Type I error rate
β	Beta: Type II error rate
C	colored suspensions
CI	confidence interval
CV	coefficient of variation
CV_i	coefficient of variation solely attributed to instrument response
d	effect size
df	Degrees of freedom
D_p	Particle diameter
EP	European Pharmacopeia
FLO	FlowCam
HIA	HIAC/Royco 9703 liquid syringe sampler
LAF	laminar air flow
LO	Light Obscuration
M	Mean
mAb	monoclonal antibody
max	Maximum
MDI	Microflow Digital Imaging
Mdn	Median
MFI	Micro Flow Imaging
M_i	Mean of a partial population
N/n	total population / partial population size
p	probability for data under validity of H0
PFS	pre-filled syringe
Ph.Eur.	European Pharmacopeia
R	reference suspension
ρ_ϕ	density of the fluid
pxl	pixel
R_i	refractive index
ρ_π	density of the particle
SbVP	sub-visible particles
sd	Standard Deviation (generally the sample-based population estimate using n-1 in the denominator)
sd^2	Sample Variance
SDVB	Styrene divinyl benzene
SE	Standard Error
SY6	Klotz Syringe with a 670nm Laser
SY7	Klotz Syringe using a 780nm Laser
T	turbid suspension
t	student t-distribution

t_{crit}	critical value of a t-distribution
USP	United Stated Pharmacopeia
V	viscous suspension
WFI	water for injection
x	particle counts

Introduction

Sub-visible particles (SbVP) analysis is considered to be a key analytical test for parenteral drug products.[8,9] The United States Pharmacopeia (USP) and European Pharmacopeia (EP) require sub-visible particle testing by light obscuration (LO) or light microscopy for parenteral products with corresponding compendia acceptance criteria.[1,3] According to the USP/EP, the LO method indicates four measurements at a volume of 5 ml (with 5 ml remaining) resulting in a total volume of 25 ml per sample.[1-3] This large sample volume makes the assay cost-intensive for biopharmaceutics. As the name - light obscuration - implies, the degree of light blockage defines the particle size (Figure 1), but the LO method has been reported to have limitations for some types of translucent particles.[10] Polystyrene particles are routinely used in calibration measurements of the LO method, however, protein particles have different shape and morphology as well as different optical properties compared to polystyrene particles.[2,6] These differences may result in difficulties in correctly detecting and accurately quantifying protein-based subvisible particles within liquid biopharmaceutical samples using the LO method.[1,6,11]

The major drawback of the standard microscope compendia methods for particle analysis is the time required, both for sample preparation and for counting and measuring size properties of the particles. In addition, sample preparation may alter the analytical readout, e.g. protein particles may theoretically dissolve during sample preparation or may be difficult to accurately detect on the filter surface. Recently, a new technique – microflow digital imaging (MDI) – has been introduced, which may be a viable add-on to assess protein-based sub-visible particles.[4-7,12] The MDI technique captures images of particles as the analyzed sample is drawn through a flow-cell centered in a field of view, resulting in particle counts, particle sizing as well as additional particle shape information (Figure 1).[11] Brightwell's microflow imaging technology (MFI) overcomes the problems of static microscopy techniques (e.g., equipment vendor claims to be able to identify and separate different particle types) by simple software

filtering of subvisible particle property values including its capabilities for counting, sizing and analyzing translucent protein aggregates and particulates.[4,6,11,13,14]

The main objectives of the first studies in this work were to assess a small volume LO method, to compare MFI and LO techniques regarding their particle counting abilities, and to evaluate MFI and a comparable technology, FlowCam, with regards to examining the morphologies of different types of particles. As non-soluble protein subvisible particles vary widely in morphology and size, it is difficult to quantitatively describe the limitations of MDI and LO for actual protein samples. Moreover real-life protein formulations also differ in optical properties such as turbidity, color, refractive index which may potentially influence SbVP detection. Further investigations were therefore made in the second part of this work to elucidate the capabilities of LO and MDI under controlled but more real-life protein formulation solution conditions.

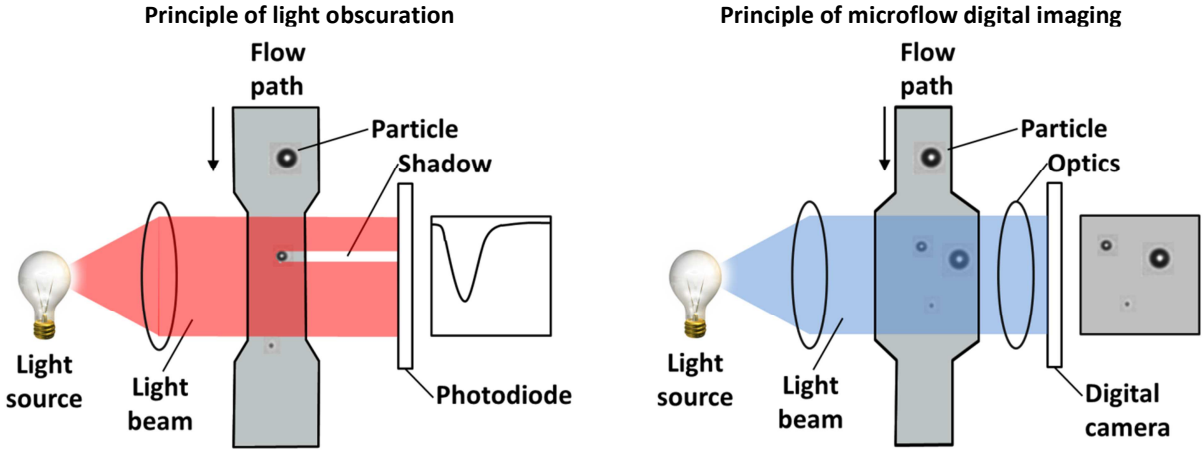

Figure 1: measuring principles of light obscuration (LO) and microflow digital imaging (MDI). Using LO the degree of light blockage defines the particle size whereas MDI technique captures images of particles as the analyzed sample is drawn through a flow-cell.

The ideal sample for detecting subvisible particles would consist of a clear, water-like fluid with individual, freely dispersed particles of moderate buoyancy and high contrast (opacity, color, refractive index) such that each particle passing between the illuminator and sensor is effectively recognized. An actual product sample that does not have the clarity and viscosity approximately equivalent to water may provide erroneous data when analyzed by LO counting method or MDI.[15,16] For example, protein formulation characteristics such as color, viscosity or inherent solution properties may provide erroneous SbVP data. Due to its high molecular weight protein represents a significant volume fraction in protein formulations. Solution non-idealities caused by protein-protein interactions in protein formulations may result in high viscosities and opalescence.[17,18] Opalescence originates from high aggregation levels, particle loads and phase separations (e.g. silicone and air bubbles). Coloration is observed in altered protein formulations and induced by degradation of absorbing amio acid residues like Cysteine, Histidine, Phenylalanine, Tryptophan and Tyrosine and reaction products with reducing sugars.

Therefore, experiments were conducted to assess the robustness of LO and MDI methods for particle counting and sizing abilities using different sample fluids. Suspensions of particles in water-based solutions were used in comparison to colored, turbid and viscous suspensions of the same particles. These suspensions were used to evaluate both particle counting and particle sizing using different sized opaque and translucent particles of both spherical and irregular shapes.

For example, in colored suspensions, the emitted light from the instrument can be absorbed by the particle and the fluid, potentially leading to relatively less light blocked by the particle than in colorless fluid. Coloration was therefore evaluated to determine if it artificially decreases the particle numbers counted by LO methods depending on the particle translucence, the overlap of the sample fluid absorbance, and the instrument emitting light wavelength. It was anticipated to only marginally

affect MDI methods because of the applied illumination optimization step (i.e., changing light intensity depending on sample properties) prior to each analysis.

With regards to solution turbidity and viscosity, the effect of these solution properties on subvisible particle counting was also evaluated. For turbidity, it was hypothesized that higher particle counts in the lower size range may be found due to noisy baselines when using MDI. Due to light scattering effects, turbidity was assumed to lower image contrast, an effect potentially leading to apparent smaller particle size measurements and lower counts. The influence of solution viscosity on the instrument's particle counting ability was hypothesized to be highly affected when a particle interaction's with light is mainly based on refraction. In addition, the effect of solution viscosity may also be dependent on the method itself: e.g., if there is a mixing phase during the beginning of the measurement, high particle counts may be observed due to the phase-mixing and potential air bubble formation, but also lower particle counts may be encountered if the specified flow rate cannot be maintained.[15] In addition, scattering effects on small particles are highly affected by the difference in refraction. Lowering the difference in refraction was assumed to lower the apparent particle size and consequently it may highly influence particle counts at the lower size limit of the analytical method.

Materials and Methods

Materials

Actual Samples

Proteinaceous Particles

Proteinaceous particles were analyzed from two monoclonal antibodies (mAb) formulations provided by F. Hoffmann-La Roche Ltd. (Basel, Switzerland), termed mAb1 and mAb2 respectively. The formulation compositions for the two different mAb samples were as follows: mAb1: 50 mg/ml in 50mM phosphate buffer (pH 6.0) and mAb2 – 10 mg/ml in 25mM sodium acetate buffer (pH 6.0). The formulation was filtered using 0.22 µm Milipak-100 Gamma Gold PVDF (Millipore, Bedford, MA, USA) and aseptically filled into pre-sterilized 20 ml glass type 1 vials (silicone-free), closed with teflon® coated 20mm serum stoppers (Daikyo Inc., Tokyo, Japan) and crimped with aluminum caps (Helvoet Pharma, Karlsbad, Germany). The mAb1 samples were stored unopened in a controlled 2-8°C stability chamber for 3¼ years. Freeze-thaw stress (-80°C/+5°C, 1 cycle) was applied to mAb1 and mAb2 samples (termed "freeze-thaw stressed"). After thawing the samples were stored at 2-8°C for 24h before analysis.

Polysorbate Related Insoluble Particles

Polysorbate related insoluble material was generated during storage of a protein solution of mAb3 (F. Hoffmann-La Roche Ltd.) at a concentration of 10 mg/ml containing 20mM citrate/sodium hydroxide buffer (pH 5.5), 190mM sucrose (Ferro, Mayfield Heughts, OH, USA), 20mM arginine-HCl (Ajinomoto, Kyobashi, Japan) and 0.02% (w/v) polysorbate 20 (Croda Inc., Snaith, UK) . These samples were prepared aseptically at a fill volume of 5.3 ml in 6 ml glass type 1 vials in the same procedure as mentioned above. Samples were stored in a controlled 2-8°C stability chamber for 17 months. The polysorbate 20 used was shown to be partially degraded and insoluble particles observed in the mAb3 solution were identified has being non-proteinaceous in nature by a staining method which is specific for proteins.[19-21]

Silicone Oil Droplets

Silicone oil droplets were obtained using a placebo solution containing 140mM sodium chloride (Merck, NJ, USA), 25mM sodium acetate trihydrate (Merck, NJ, USA), 100mM benzyl alcohol (Sigma Aldrich, St. Luis, Missouri, USA), 0.05 % (w,v) polysorbate 80 (Croda Inc., Snaith, UK), 10mM glacial acid acetic (pH 6.0). The placebo solutions were stored in staked-in needle pre-filled syringe (PFS) (Gerresheimer, Düsseldorf, Germany), containing sprayed in silicone, in a temperature controlled stability chamber at 25°C for 6 months.

Negative and positive controls were utilized at each testing session to ensure that the environment, sample preparation procedure, and instrument were all suitable for the analysis.

Particle Standards

Dilution Media for Particle Standards

Various types of particle standards were utilized for the comparison of the MDI and LO techniques in terms of particle sizing and counting capabilities. In order to stabilize the particle suspensions, a surfactant containing dilution media was used containing 0.02 % (w/v) polysorbate 20 (Croda International, Snaith, England) in freshly drawn water for injections (WFI, distilled internally). This solution, termed “dilution media”, was sterile filtered using 0.22 µm Stericup-GV Filters (PVDF) membrane type (Millipore, Massachusetts, USA).

Polystyrene Particles

Polystyrene particles NIST particle size standards were obtained from Thermo Scientific (Fremont, CA, USA) with nominal particle sizes of 2, 5, 10 and 25 µm. Polystyrene particles NIST count standards were obtained from Thermo Scientific (Fremont, CA, USA) with nominal particle sizes of 2, 5, 10 and 25 µm and concentrations of 2000 particles per ml as summarized in Table 1.

Table 1: Summary of physical properties of polystyrene particle standards

cat no	nominal size	certified mean diameter D_p	standard deviation sd	uncertainty mean diameter	microsphere density ρ_p	index of refraction	approximate concentration
	[µm]	*[µm]*	*[µm]*	*[µm]*	*[g/cm³]*	at 589nm	
4202	2	1.999	0.022	0.02	1.05	1.59	0.44% solids
4205	5	4.987	0.05	0.04	1.05	1.59	0.31% solids
4210	10	10.00	0.09	0.08	1.05	1.59	0.23% solids
4225	25	25.09	0.12	0.38	1.05	1.59	0.53% solids
6002	2	1.998	0.022	0.02	1.05	1.59	2000/ml ± 10% ≥1.3µm
6005	5	5.010	0.035	0.05	1.05	1.59	2000/ml ± 10% ≥3µm
6010	10	10.00	0.05	0.09	1.05	1.59	2000/ml ±10% ≥7.5µm
6025	25	25.09	0.12	0.38	1.05	1.59	2000/ml ±10% ≥15µm

Each particle size standard suspension was diluted with dilution media to a stock concentration of approx. 13000 /ml using the following relation:

Equation 1: suspension based particle concentration determination

$$\frac{x}{V} = \frac{6\rho_f}{\pi D_p^3\left(\rho_f + \frac{\rho_p}{C} - \rho_p\right)}$$

Where x/V represents the particle concentration, ρ_f the fluid density, ρ_p the particle density, C the suspension's particle concentration in percent solids and D_p the particle's mean diameter. The stock suspensions (free of foreign particles or particle fragments) were tested by LO and MDI methods to assure the particle stock suspensions can be mixed without having particle population overlaps.

For verification of the small volume LO method, polystyrene size standards with nominal particle size of 2, 10 and 25 µm were used whereas each particle standard was diluted with water for injection (WFI) to three different concentrations: 260, 360 and 2200 counts per ml for 2 µm particles, 25, 75 and

330 counts per ml for 10 µm particles and 5, 20 and 120 counts per ml for the 25 µm particles (termed "Polystyrene Particles 1").

To compare the limitations of MDI technologies, Polystyrene particle count standards in a range of 2, 5, 10, 25 µm with particle concentrations of 2000 ± 200 per ml (termed "Polystyrene Particles 2") were also prepared.

For assessing sample matrix influence, a mixture of 2, 5 and 10 µm polystyrene size standard stock suspensions was compounded containing 4333 particles per ml by calculation for each particle population.

Glass Particles

Borosilicate glass particle standards were used as powders from Thermo Scientific (Fremont, CA, USA) with nominal particle sizes of 2 and 8 µm as summarized in Table 2.

Table 2: Summary of physical properties of borosilicate glass particle standards

Cat no	nominal size [µm]	certified mean diameter [µm]	standard deviation [µm]	uncertainty mean diameter [µm]	microsphere density [g/cm^3]	index of refraction at 589nm	approximate number per gram per gram
9002	2	2.00	0.6	0.4	2.50	1.56	9.5E+10
9008	8	8.00	1.0	0.4	2.55	1.56	1.5E+09

Suspensions of approx. 13000 /ml were obtained by suspending the glass particle powder (C=1) with diluent media using the simplified relation:

Equation 2: powder based particle concentration determination

$$\frac{x}{V} = \frac{6\rho_f}{\pi D_p^3}$$

Where x/V represents the particle concentration, ρ_f the fluid density, ρ_p the particle density, and D_p the particle's mean diameter. A mixture of 2 and 8 µm glass particle stock suspension was compounded containing 6500 particles per ml by calculation for each particle population.

"False Protein Standard"

False protein aggregate standard were obtained from Fluid Imaging Technologies (Fluid Imaging Technologies, Maine, USA) with nominal particle concentrations of 5383 /ml ±12% >25 µm, 8818 /ml ±12% >10 µm (according to vendor information). The sample was re-suspended by gently inverting 20 times prior to any dilution step. The received material is considered to be under development by the supplier, therefore, stability parameters have not yet been established and further information about the manufacturing of the standard was not disclosed.

Colored Suspensions

A melanoidine containing solution (manufactured internally) was filtered using 0.22 µm Stericup-GV Filters (PVDF) membrane type (Millipore, Massachusetts, USA). The stock solution was prepared to mimic real life protein formulations: i.e., similar absorption spectra to that of altered or degraded protein formulation solutions can be expected. The samples were compounded using dilution media to create a target coloration defined by the European Pharmacopeia as B1.[22] The calculated

particle concentration for polystyrene particle containing samples was 1000 counts per ml and the population for glass particle containing sample suspensions was 3000 counts per ml.

Turbid and Viscous Suspensions

A turbidity standard based on styrene divinyl benzene (SDVB) copolymer beads in the submicron range was used to obtain turbid suspensions. NIST traceable AMCO CLEAR Turbidity Standard 1000 FTU (GFS Chemicals, Ohio, USA) was filtered sterile using 0.22 µm Stericup-GV Filters (PVDF) membrane type (Millipore, Massachusetts, USA) . Viscous suspensions were compounded using analytical grade Glycerol (ACROS, Geel, Belgium), filtered through 0.22 µm Stericup-GV Filters (PVDF) membrane type (Millipore, Massachusetts, USA).

Turbid and viscous particle suspensions were compounded by mixing polystyrene, glass and "false protein particle" stock suspensions with above solutions to target turbidity values of 15 and 30 FTU and viscosities of 1, 11 and 20 mPa*s. Due to the change in refractive index, glycerol quenches turbidity caused by SDVB submicron particles. Therefore the needed amount of SDVB copolymer beads in glycerol-water mixtures was assessed prior compounding (Figure 2) to obtain target turbidity values.

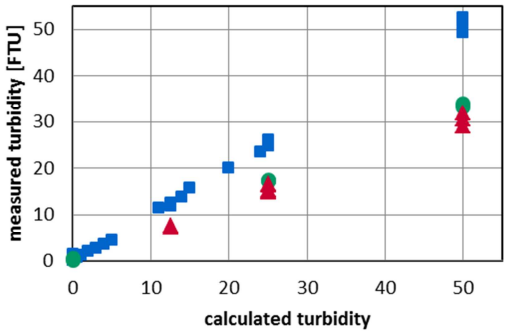

Figure 2: Turbidity in glycerol/water mixtures: measured turbidity vs. theoretical turbidity using mixtures of SDVB beads with water (■) and water/glycerol with a refractive index of 1.42 (●) and 1.43 (▲). The slope for water like suspensions is 1.01 whereas the slopes are 0.66 and 0.61 for glycerol/water mixture of 10mPa*s and 20mPa*s, respectively.

The final particle suspensions theoretically contained 3000 particles per milliliter for polystyrene particles, i.e. 1000 particles per milliliter of 2 µm polystyrene size standard, 1000 particles per milliliter for 5 µm polystyrene size standard and 1000 particles per milliliter 10 µm polystyrene size standards. The final glass bead suspensions theoretically contained 3000 particles per milliliter of the 2 µm glass particles and 3000 particles per milliliter of the 8 µm glass beads (in total 6000 particles per milliliter). The "false protein particle standard" theoretically contained particle concentrations of 1345 /ml >25 µm and 2204 /ml >10 µm.

Analytical Methods

Turbidity Determination

Under laminar airflow (LAF) conditions, samples were prepared by transferring the solution into washed and sterilized, particle-free 11mm glass cuvettes (Hach Lange GmbH, Düsseldorf, Germany). Using a HACH 2100AN turbidimeter (Hach Company, Loveland, CO), the turbidity measurements was performed instrumentally as outlined in the EP method 2.2.1.[23]. The instrument was calibrated against formazin reference suspensions and thus the results are expressed as formazin turbidity units (FTU).

Viscosity Measurement

Samples viscosity was assessed by a MCR300 rheometer (Anton Paar GmbH, Graz, Austria) using a plate-cone measurement system (Cone: CP25-0.5 Anton Paar GmbH, Graz, Austria). Measurements were performed at 20°C. Sample was equilibrated for one minute at a shear rate of 10-s, then shear rate was increased from 100-2000-s within one minute. Finally during the holding step at a shear rate of 2000-s dynamic viscosity was recorded six times over 15 seconds. The averaged value is the result of a single measurement. Measurements were done as duplicates reporting the mean ± absolute deviation.

Color Determination

Using a Dr. Lange LICO 200 liquid colorimeter (Hach Company, Loveland, CO), the coloration of the samples was determined in 11mm glass cuvettes (Hach Lange GmbH, Düsseldorf, Germany). The spectral data of sample absorbance between 380 and 720 nm in 10 nm steps was transformed into Lab-values which also can be described in European Pharmacopeia (EP) and United States Pharmacopeia (USP) color codes.[22]

Absorbance Spectroscopy

The sample absorbance was determined by measuring UV-visible absorption spectra between 320 and 840nm on a UV/Vis Spectrometer (Lambda 35, Perkin Elmer, Waltham, Massachusetts, USA) using 1cm plastic disposable cuvettes.

Refractometry

The refractive indices were collected using a Mettler RE40D digital refractometer at 20°C.

Light Obscuration

The sub-visible particle counts were measured using the different light obscuration methods as described below. The subvisible particles are detected and their size deduced from the amount of light blocked as the particles pass a light beam.

HIAC/Royco

The analysis was performed using a HIAC/Royco 3000A Liquid Syringe Sampler (termed HIAC) with a HRLD-150 sensor with a 780 nm laser light (max. particle concentration 18,000/ml as per the vendor's information) and the software PharmSpec version 2.0 (HACH Ultra Analytics, Grant's Pass, OR) under laminar air flow (LAF) conditions. Fill and ejection rates were fixed to 10 ml/min.

For the regular USP/EP method, sample measurement consisted of four injections/aliquots at a volume of 5 ml each.[1,3] For the small sample volume LO method, each sample measurement was performed three times at a volume of 0.4 ml, using a modified version to USP/EP method, as described previously.[3,24] The first injection was discarded and the mean value was obtained from the last two injections for the small sample volume method compared to the mean value of the last three injections was calculated for compendial test methods.

Discarding the first run with 0.4 ml method was not sufficient for the high viscosity samples used when assessing the sample matrix influence (Figure 3). Therefore, 4 aliquots of 0.4ml were used per sample analysis, whereas the first two were discarded and the mean value was calculated from run 3 and 4. Between each sample analysis, the system was rinsed with water for injection to the point at which the ≥2 µm particle counts of the apparatus were less then 10 to avoid the influence of environmental contaminations during the measurements. Sub-visible particle are presented as cumulative counts per ml.

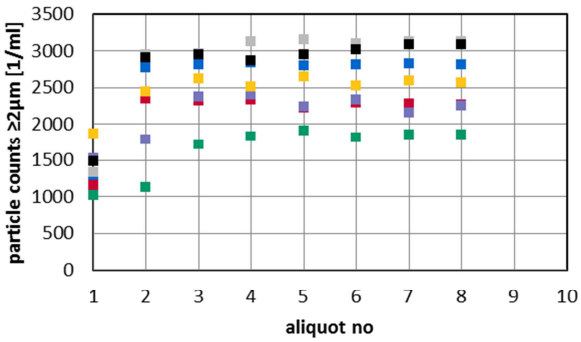

Figure 3: Subvisible particle counts (≥2 µm) as measured by low volume LO method (0.4 ml aliquots) for 2, 5, 10 µm polystyrene beads in different sample matrices: water as reference media R(■), colored matrix C(■), opalescent matrix T(■), 35 FTU at 11 mPa*s TTV (■), 30 FTU at 20 mPa*s TTVV (■), 16 FTU at 20 mPa*s TVV(■) and clear at 11 mPa*s V(■). See Table 5 for further description of sample matrices.

Klotz Syringe 670nm and Syringe 780nm

A different light obscuration system called Syringe (Fa-Klotz, Bad Liebenzell, Germany) was also used to perform subvisible particle analysis. *Two 230 µm* Flow Cells with a LDS23/25 sensors with a maximum particle concentration of 100000 /ml were tested. One with a 670 nm laser ligth source (termed SY6) and similar to the used HIAC sensor one with 780 nm laser (termed SY7) light. In analogy to HIAC measurements, fill and ejection rates were fixed to 10ml/min and each sample measurement was performed four times at a volume of 0.4 ml per injections. The first two runs were discarded and the mean value was obtained from injection 3 and 4. Between each sample analysis, the system was

rinsed with water for injection to the point at which the ≥ 2 µm particle counts of the apparatus were less then 10 to avoid the influence of environmental contaminations during the measurements.

Microflow Digital Imaging

MFI 5x

Sub-visible particles were measured using MFI DPA4100 Flow Microscope Series B (Brightwell Industries, Ontario, Canada) under LAF conditions. The instrument can be configured either for a particle size range of 0.75 to 100 µm for the 14x magnification or 2 to 400 µm for the 5x magnification. Brightfield images of individual particles are captured as a sample stream passes trough a flow-cell centered in the field of view illuminated by a blue LED. Images are analyzed by the system software (DPA4100 MFI software, version 6.9.7) to extract each particle and compile a database containing particle counts and size. Additionally, saved images can be analyzed retrospectively to determine count, size and transparency, as well as shape parameters such as area, perimeter, circularity, maximum Feret's diameter (expressed in microns), and aspect ratio (ratio of the minor axis length over the major axis length of an ellipse with the second moments of the particle). Transparency is expressed as mean object intensity which stands for the average intensity of all pixels representing a particle. These intensity levels that are related to 10bit sensor of the digital camera, which provides 1024 illumination levels between dark (0) and bright (1023). This property is affected by the difference between refractive index of the particle and the background. The circularity of an object is expressed as a value between 0 and 1 and represents the ratio of the circumferrence of an equivalent spherical diameter (ESD) area over the measured perimeter. The samples were drawn under LAF from a 5 ml pipette through the flow-cell using a peristaltic pump. Prior to each analysis, WFI was flushed trough the system to provide a clean baseline and to optimize the illumination. For each sample, three separate runs of each 0.4 ml were analyzed in parallel to the adapted LO method, whereas the first run was discarded and the remaining

two were use for calculation. Additionally, one picture per second was captured for the shape analysis whereas the pictures of the first run were also discarded.

For testing the influence of the sample matrix, sub-visible particles were measured using a newer MFI instrument: MFI DPA4200 Flow Microscope Series B (Cell Biosciences, Inc., California, USA; former: Brightwell Technologirs Inc., Ontario, Canada). The instrument uses a 5 fold optical magnification and a 100 µm field of view flowcell. Images of individual particles are captured as a sample stream passes trough a flow-cell centered in the field of view illuminated by a blue LED. Images were analyzed by the system software (MVSS software, version 1.2) to extract each particle and to compile a database containing particle counts and size. A continous flow was obtained using a peristaltic pump. Prior to each analysis, the flow cell was cleaned by flushing alternately with WFI and 2-propanol and subsequently allowing the system to run dry. A sample volume of 1.2 ml was drawn under LAF using a 2.5 ml pipette whereas 0.18 ml sample was used to flush the flowcell and approx. 0.17 ml was used to optimize the illumination and substract the flow cell background. For each sample 0.80 ml was analyzed. Additionally, approximately three pictures per second were captured and saved for the shape analysis.

FlowCam 10x

Subvisible particle counting and shape analysis was also performed using the FlowCam benchtop system with a colored camera and 10x magnification (Fluid Imaging Technologies Inc., Maine, USA) and the respective system software (VisualSpreadsheet software, version 2.4.10). FlowCam uses a similar technology that to the MFI instrument but utiilizes a white LED light source, crops particle images automatically and uses a 1ml syringe pump to establish continous and flow. Similar to MFI measurements, the system was cleaned flushing alternately with WFI and 2-propanol prior to each sample. Of the 1.2ml sample, 0.3 ml were used to flush a 80µm FC80FV field of view flow cell. Background substraction was peformed using the first data frames. For each sample 0.8 ml was

analyzed. Particle segmentation was performed using a dark threshold of 25. The distance to the nearest neighbour was set to 3 microns. FlowCam 10x, auto image frame rate and flash duration were set to 20 frames per second and 19 microseconds, respectively.

An overview of key instrument parameters for the subvisible particle counting methods used in this work is provided below in Table 3.

Table 3: Overview of light obscuration (LO) and microflow digital imaging (MDI) methods for measuring subvisible particles

	Microflow Digital Imaging (MDI)				**Light Obscuration (LO)**				
	FlowCam 10x	**dpa4200 MFI 5x**	**dpa4100 MFI 5x**	**dap4100 MFI 14x**	**HIAC**	**HIAC**	**HIAC**	**Syringe 670nm**	**Syringe 780nm**
Abbrev.	FLO	MFI	MFI 5x	MFI 14x	EP / USP[1-3]	small sample volume	HIA	SY6	SY7
Optical Magnification	10x	5x	5x	14x	N/A	N/A	N/A	N/A	N/A
Light source	White LED	Blue LED	Blue LED	Blue LED	780nm Laser	780nm Laser	780nm Laser	670nm Laser	780nm Laser
Sample volume used prior to analysis / Tare volume	0.3	0.35	0.35	0.35	0.1	0.1	0.1	0.1	0.1
*Particle Size Range**	5-1000µm	1-70µm	2.25-400 µm	0.75-100µm	1.2-150µm	1.2-150µm	1.2-150µm	1-50µm	1-50µm
Analyzed Sample Volume	1 x 0.8ml	1 x 0.8ml	3 x 0.4ml	3 x 0.4ml	4 x 5ml	3 x 0.4ml	4 x 0.4ml	4 x 0.4ml	4 x 0.4ml
Result=Average from aliquot no.	1	1	2 & 3	2 & 3	2, 3 & 4	2 & 3	3 & 4	3 & 4	3 & 4
Flow Rate	0.2 ml/min	0.17 ml/min	0.2 ml/min	0.1 ml/min	10 ml/min	10 ml/min	10 ml/min	10 ml/min	10 ml/min
Approx. Sampling efficiency	14%	31%	85%	8%	100%	100%	100%	100%	100%
Syringe Size	1ml	N/A	N/A	N/A	10ml	10ml	10ml	5ml	5ml

*according to vendor information N/A – not applicable

Results and Discussion

Small Sample Volume LO Method Verification

The scope of this first study was to compare a small sample volume method for light obscuration to the larger volume compential test. The development of a smaller volume LO method is warranted in order to be able to employ a material saving LO method, especially for pharmaceutical dosage form development purposes. As an initial step, three different polystyrene particle suspension standards ("polystyrene particles 1") of particle size ranges of 5, 10 and 25 µm at three different concentrations were used. The comparison of results from the small sample volume LO method and the compendia tests USP <788> and EP 2.9.19 is presented in Figure 4. Counting accuracy data obtained with the particle standards with the small volume and compendia methods were quite comparable. The results were subjected to a T-test which showed that the small sample volume method was not significantly different from the USP/EP method at a confidence level of 99% for all tested determinations.

As a second part of this study, the small volume LO method was further verified by measuring particle counts in actual aged protein solutions – mAb2 and mAb3 (Figure 5). The results for the small sample volume method were not statistically different from the EP/USP method at a confidence level of 99% for mAb3, and comparable for the mAb2, both having been stored for 6 years at 2-8°C. Although in the case of the mAb2 experiments, the differences for particles ≥ 10 µm were statistically significant for these samples, these difference are not considered of practical relevance due to (1) the low level of subvisible particles (33 vs. 48 particles), and (2) given the typical method variability of light obscuration observed over time in the analytical laboratories.

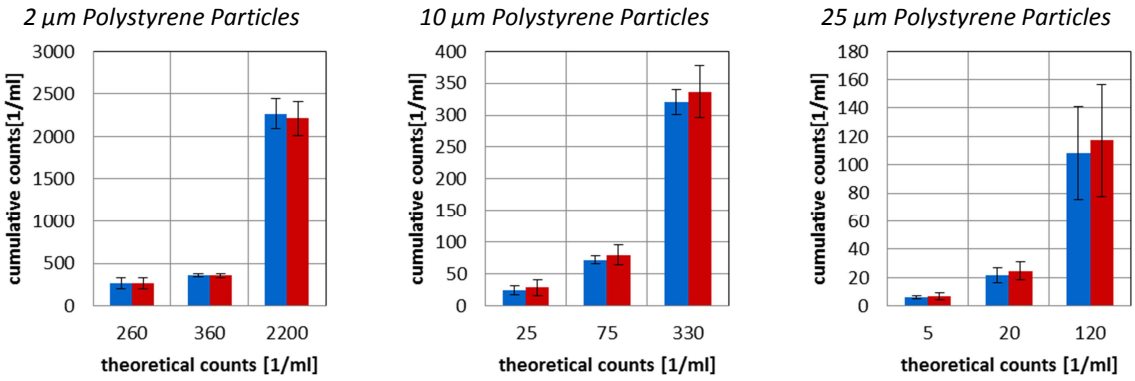

Figure 4: Comparison of counting accuracy of USP/EP and small sample volume LO methods using polystyrene standards with a nominal size of 2 µm, 10 µm and 25 µm (polystyrene particles 1). The error bars represent ±σ of n=6 independent measurements. USP/EP method (■), small sample volume method (■).

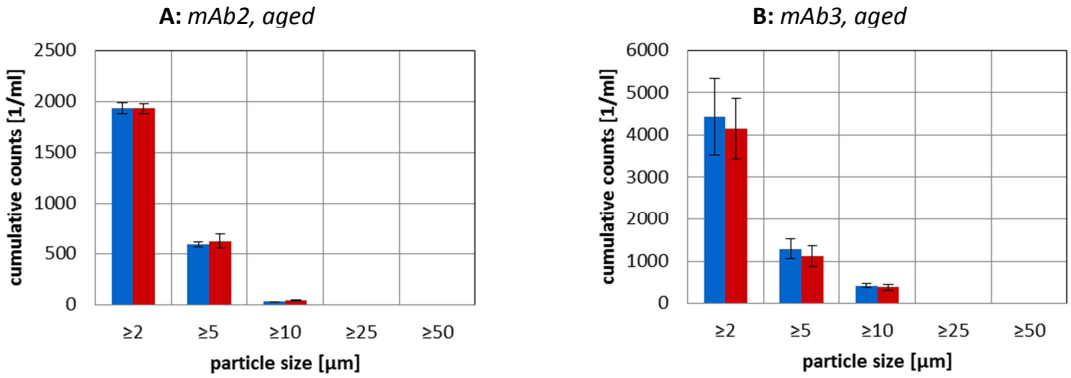

Figure 5: Cumulative particle counts at ≥ 2, 5, 10, 25 and 50 µm as measured by two LO methods in (A) aged mAb2 formulations and (B) aged mAb3 formulations. The error bars represent ±σ of n=6 independent measurements. USP/EP method (■), small sample volume method (■).

One of the most important experimental parameters for developing a reproducible small sample volume LO method is to ensure that the volume of the first aliquot to be measured is sufficiently higher than the sum of dead and the mixing phase volumes during sample introduction. This minimal volume is needed to avoid false positive results from being generated during the initial measurement. These parameters are dependent on the sample type, for example during the mixing phase, streaking can occur which could lead to false positive particle counting [25]. Therefore, the small sample volume method was also tested with a large number of aliquots of 0.4 ml for every sample. These results (Figure 6) showed that a pre-dispensed volume of 0.4 ml is sufficient for all measured samples.

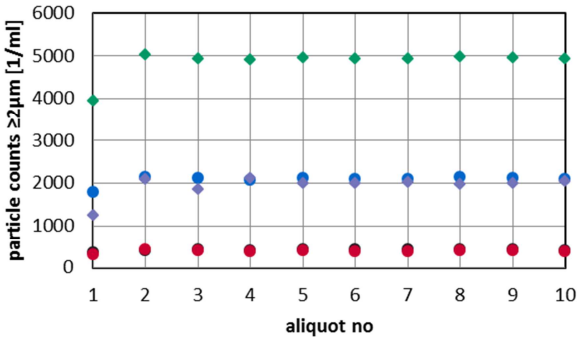

Figure 6: HIAC small sample volume LO method showing particle counts ≥ 2 µm versus number of 0.4 ml aliquots for a variety of samples: polystyrene particle bead standards in suspension, 2 µm (●), 10 µm (●), and 25 µm (●), and protein samples containing aged mAb2 (●) and aged mAb3(●).

In summary, the small volume LO method yields comparable results to the USP/EP LO methods in terms of the particles counts at ≥ 2, ≥ 5 µm as well as for the counts for USP/EP ≥ 10, ≥ 25 µm. In addition, the small sample volume LO method applied requires only 6% sample volume USP and EP defined LO methods.

Exploring the Advantages and Limitations of MDI

Comparison of Light Obscuration and Micro Flow Imaging

Polystyrene particle bead standards ("polystyrene particles 2") were used initially to compare particle counting accuracy and precision of two different sub-visible particle instruments (MFI and LO). Using particle standards with a nominal size of 2, 5, 10 and 25 µm (EZY-CAL NIST polystyrene particle size standards Thermo Fisher), the objective of the first study was to compare LO and MFI versus the label claimed particle concentration of 2000±200 particles per ml (Figure 7). For 10 and 25 µm particles, both MFI (5x magnification) and LO counts were within the expected range and were comparable with regards to accuracy and precision. For 5 µm particles, the MFI (5x and 14x magnification) and LO counts were within the expected range. However, the precision of the MFI using a high magnification setting was poor compared to either the MFI using a low magnification setting or the LO instrument. Low sample efficiency implies a lower probability to coincidentally meet the true mean value compared to high sample efficiencies. Additionally, with increasing efficiency (meaning increasing probability of detecting particles), the confidence interval decreases. It can therefore be stated that assay precision for particle counting can be indirectly proportional to sample efficiency which for LO is 100%, for MFI 5x magnification 85%, and for MFI 14x magnification only 8%.

In addition, the MFI counts (5x magnification) were slightly higher than the LO counts which might be attributed to the resolution at the lower size range limit. MFI resolution is limited by the optical system and the sensor. The sensor provides an image of 1280 x 1024 pixels (1.3 megapixel) which corresponds to a field view of 1760 x 1400 µm for MFI 5x magnification and 620 x 500 µm for MFI 14x magnification. Consequently, the pixel density of MFI 5x magnification is 1.895 µm/pxl and 0.238 µm/pxl for MFI 14x magnification. For 2 µm particles, the MFI counts using the high magnification was slightly above the expected range which also could be explained by the resolution, as mentioned above,

whereas the LO counts were within the expected range. Using actual protein formulation samples, such as a freeze-thaw stressed mAb2 solution, the MFI counts were generally higher compared to the LO results for subvisible protein particles up to 25 µm (Figure 9 and Figure 10). This result has also been reported previously for other proteins although the discrepancy was not as pronounced.[6] Surprisingly, MFI 5x counts in the particle size range of 2.25 to 3 µm were substantially higher than MFI 14x counts for well-defined polystyrene particles and protein samples (Figure 8 and Figure 10), respectively. These subvisible particle counting discrepancies at low size ranges for proteinaceous particles may be explained by how the particles are recognized by the different technologies. MFI software computes whether a pixel is "particle" or "not particle" based upon a defined threshold value for the difference of background pixel value subtracted from incoming value of the same pixel. For particles with sizes of a single pixel, static intensity irregularities resulting from the light source, the sample liquid, the flow cell or the magnification system could cause false counting and ghost particles. In addition, software caused particle fragmentation may lead to significantly higher particle counts in the 2µm size range, but only affect particle counts in larger particle size regions to a minor extent.

It has been hypothesized and confirmed experimentally in the literature that the LO method may have difficulties in counting translucent subvisible particles since light is only partially blocked by translucent particles (such as glass or proteinaceous particles) as compared to polystyrene particle of the same size which are not translucent in nature. Therefore, the LO technique may under count and/or recognize translucent particles as smaller in size than they are in reality. Reasons for counting discrepancies between MFI and LO hypothesized in the literature include differences in the translucence and circularity of protein particles in comparison to polystyrene standards[6].

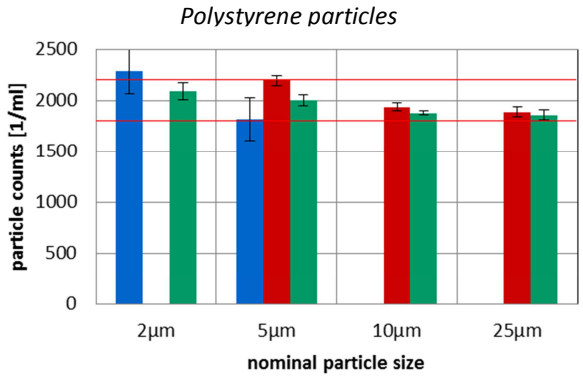

Figure 7: Particle counting accuracy of LO (HIAC, ■), MFI 5x magnification (■) and MFI 14x magnification (■) for polystyrene particle bead standards. Particle counts are within the specified limitations of the polystyrene counting samples. The error bars represent ±σ of n=3 independent measurements

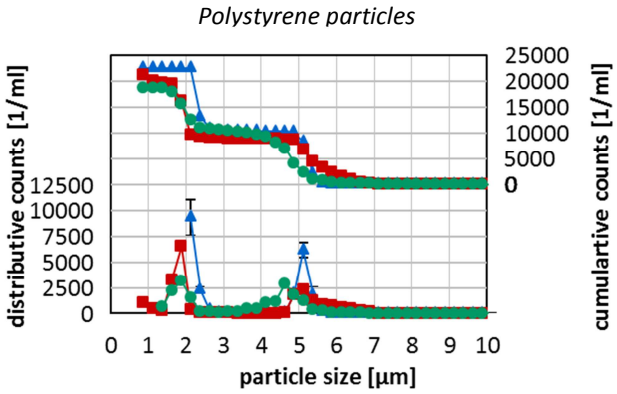

Figure 8: Particle counting accuracy of LO (HIAC, ●), MFI 5x magnification (▲) and MFI 14x magnification (■) for polystyrene particle bead standards. Distribution of 2 and 5 µm polystyrene beads with resolution by particle size. The error bars represent ±σ of n=3 independent measurements.

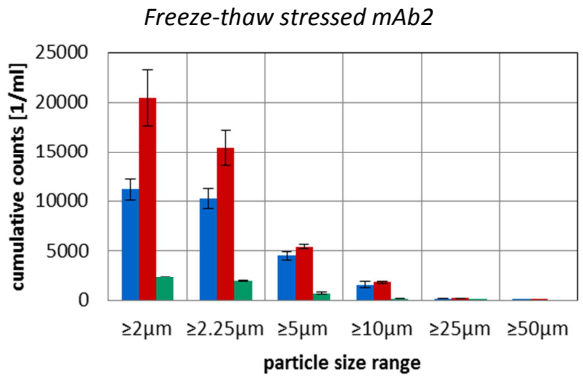

Figure 9: Particle counting of freeze-thaw stressed mAb2 samples as measured by LO (HIAC, ■), MFI 5x magnification (■) and MFI 14x magnification (■). Cumulative particle counts with standard bins. The error bars represent ±σ of n=3 independent measurements

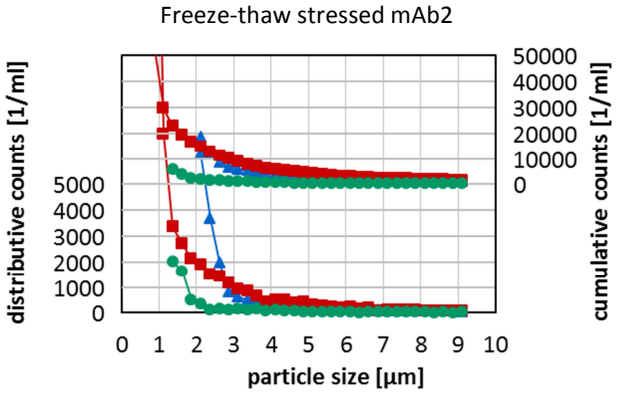

Figure 10: Particle counting of freeze-thaw stressed mAb2 samples as measured by LO (HIAC, ●), MFI 5x magnification (▲) and MFI 14x magnification (■). Distributive and cumulative particle counts below 10µm.The error bars represent ±σ of n=3 independent measurements.

Comparison of Micro Flow Imaging (MFI) and FlowCam

Particle shape and morphology were evaluated with the MFI (5X and 14X) and FlowCam (10X) instruments for a variety of subvisible particles including polystyrene bead standards, silicone oil droplets, aged and stressed protein samples, and polysorbate related particles. FlowCam 10x pictures were generally of better quality than MFI 5x and even MFI 14x pictures. The captured images of the different types of subvisible particles support the results and conclusions drawn from the shape analyses below (Table 4).

As shown in Figure 11, the results for the chosen shape parameters were dependent on the particle size range for both MFI 5x and FlowCam 10x. The FlowCam 10x instrument showed higher variability than the MFI 5x instrument with regards to mean object intensity and circularity, presumably due to a different depth of field (Figure 11). For particles < 10 µm, the MFI at 5x magnification could not distinguish between the particle types analyzed, namely polystyrene particles, silicone oil droplets, proteinaceous particles or polysorbate related particles (Figure 11). Using the shape parameter "mean intensity", MFI 5x could only reliably distinguish between silicone oil droplets and proteinaceous sub-visible particles for particle sizes > 10 µm, although the differences detected were rather marginal. In fact, the circularity of silicone oil droplets and proteinaceous sub-visible particles were not significantly different. Using the shape parameter "circularity", FlowCam 10x could clearly separate silicone oil droplets from proteinaceous sub-visible particles for particle sizes > 5 µm (Figure 11). On the other hand, proteinaceous particles could not be distinguished from excipient-related particles using the single shape parameters "mean intensity" and/or "circularity" (Figure 11). Because MFI 14x has low sampling efficacy, fewer data points could be calculated. High standard deviations were obtained due to blurred images resulting from a combination of low depth of field and the large depth of the flow cell for the MFI 14x instrument.

Previous reports have confirmed differences using MFI mean object intensity (surrogate for translucency) of protein particles versus polystyrene standards for particles sizes ≥ 5 µm (as shown in Figure 11).[6] However, MFI circularity measured was not significantly different for all particle sizes observed. Thus, for particle sizes ≥ 5 µm, the reason for counting differences between MFI and LO may be the difference in translucency for protein particles, but not necessarily due to a difference in the measured circularity. The translucency measured of 2 µm protein particles was similar, however, to the translucency of polystyrene standards of similar size (Figure 11). Thus, the reason for the obsereved counting differences between MFI and LO for particles in the range of 2 to 5 µm cannot be solely attributed to the apparent differences in the translucent nature of protein particles. The translucency and circularity of polysorbate 20 related particles was measured similar to polystyrene standard for particle size ≤ 15 µm (Figure 11). Nevertheless, the MFI counts were significantly higher for particles ≥ 2 and ≥ 5 µm. Thus, translucency and circularity cannot be the (sole) reason for counting differences between MFI and LO.

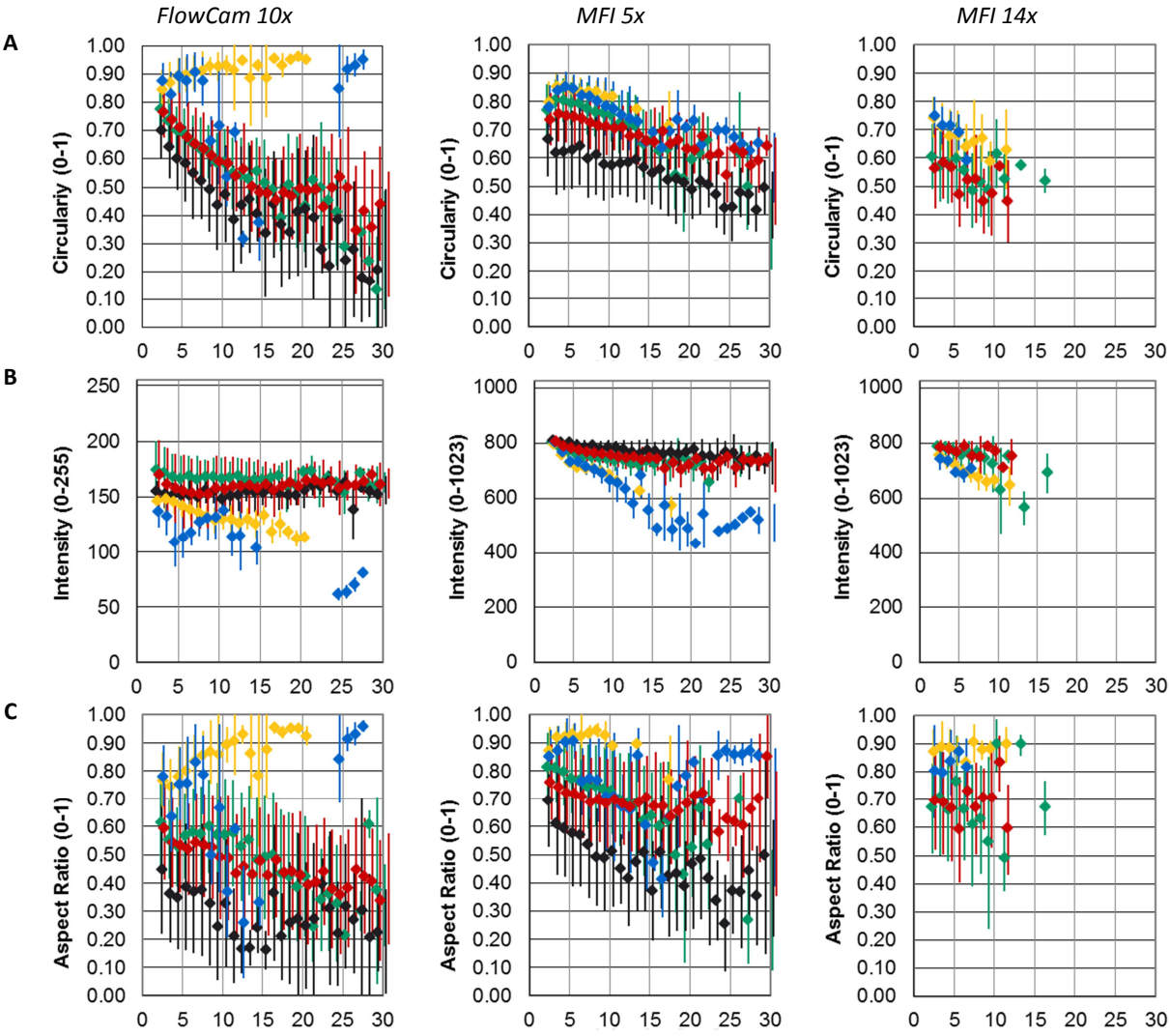

Figure 11: Particle shape as measured by FlowCam and MFI analyzed by instrument software: (A) Circularity, (B) Mean Intensity and (C) Aspect ratio. Polystyrene particle standards 2 [EZY CAL 2, 5 10, 25um] (◆), silicone oil droplets mAb4 placebo (◆), freeze-thaw stressed mAb2 (◆), aged mAb1 (◆), polysorbate related particles mAb3 (◆). The error bars represent ±σ of ≥ 20 representative particles.

An “aspect ratio” particle analysis for MFI 5x was described previously in literature to effectively isolate silicone oil droplets greater than 5 µm in size.[25,26] The published data analysis approach of using a “silicone oil filter of ≥0.85 aspect ratio” was applied to the different particle populations evaluated in this work (Figure 12). In Figure 12, the total number of particle counts of the individual population was normalized to 100%, and the shaded parts represent particles with an aspect ratio ≥0.85. In general, particle counts increased with decreasing particle size implying the data analysis filter was neither applied nor suited for 40 to 85 % of the particles detected. Within the size range of 5 to 10 µm, the data analysis filter isolated 98% of the silicone oil droplets yet only 13 % of its whole population. When the data analysis filter was applied to proteinaceous particles within the same size range, a misclassification of 18 % (mAb1) and 26 % (mAb2) was observed, respectively. At higher size ranges, the particle numbers are in general too low to draw utilizable conclusions for the total particle population.

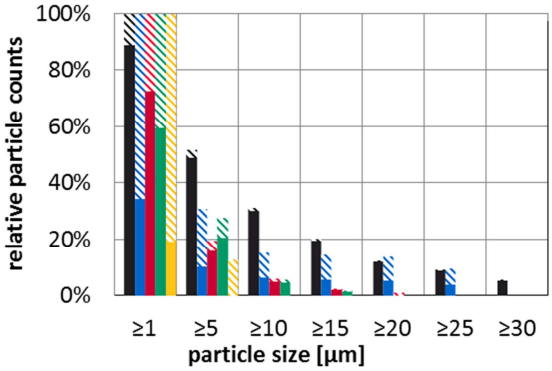

Figure 12: A “silicone oil filter” to analyze the aspect ratio of various particle samples as a function of different particle size populations as measured by MFI 5x. The total number of particles for each sample was normalized to 100%. The dashed bars represent the fraction of particles which show aspect ratio values >=0.85, the solid bars represent the fraction of particles with aspect ratio values of <0.85. Samples include Polystyrene particle standards 2 [EZY CAL 2, 5 10, 25um] (■), silicone oil droplets mAb4 placebo (■), freeze-thaw stressed mAb2 (■), aged mAb1 (■), polysorbate related particles mAb3 (■).

Table 4: Representative images of different subvisible particles as measured by MFI and FlowCam

	FlowCam 10x	MFI 5x	MFI 14x
Polystyrene size standards	 3µm  4µm  10µm  26µm	2µm  5µm  10µm  25µm	 2µm  5µm  10µm No adequate picture captured
Silicone Oil Droplets	 3µm  5µm  12µm  26µm	2µm  5µm  10µm  26µm	 2µm  6µm  10µm  19µm
Excipient related particles	 3µm  6µm  12µm 	2µm  6µm  11µm  25µm	 2µm  6µm  12µm 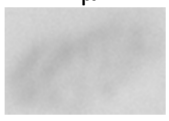 20µm

	FlowCam 10x	MFI 5x	MFI 14x
Proteinaceous particles (mAb1)	 3µm  5µm  11µm  25µm	2µm  5µm  10µm  26µm	 2µm  6µm  11µm 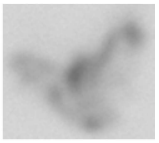 21µm
Proteinaceous particles (mAb2)	 3µm  5µm  11µm  26µm	2µm  5µm  10µm  25µm	 2µm  5µm  11µm 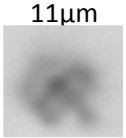 18µm

Sample Matrix Influence

Determination of Sample Properties

Prior to the analysis of different subvisible particulates in solutions with varying physcial properties, samples were first analyzed and catorgoriezed in terms of their different solution properties by assessing color, turbidity, viscosity, refractive index and their UV-absorption spectrum. Different solutions were prepared with different physical properties and in general they showed the expected variety of physical properties (Table 5 and Figure 13). However, it is worth noting that turbidity had a significant impact on the color determination. Due to high turbidity levels, the solution appeared darker and consequently was attributed to best match a slightly different color standard (Table 5).

Table 5: Physical properties of different sample suspensions including the water reference, colored, turbid and viscous solutions.

	Abbrev.	Color[22,27]	Refractive Index Index	Viscosity [mPa*s]	Turbidity[23] [FTU]
Water Reference Suspension	R	B9	1.3346±0.00095	1.0±0.0	0.0±0.1
Colored Suspension	C	B1	1.3345±0.00087	1.0±0.0	0.9±0.1
Opalescent Suspension	T	B6	1.3346±0.00089	1.0±0.0	51.1±0.9
Viscosity level II /opalescence level I suspension	TVV	B7	1.4262±0.00020	20.2±0.2	16.2±1.2
Viscosity level II /opalescence level II suspension	TTVV	B6	1.4262±0.00000	20.2±0.1	31.3±1.4
Viscosity level I /opalescence level II suspension	TTV	B6	1.4189±0.00632	11.7±0.1	34.2±0.5
Viscous suspension	V	B9	1.4190±0.00581	11.0±0.1	1.0±0.3

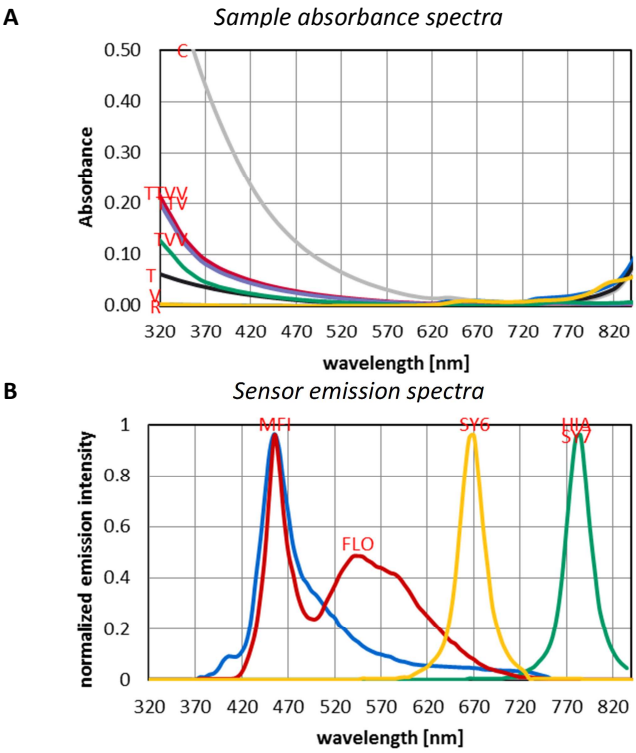

Figure 13: (A) UV Absorption spectra for particle free sample matrices including water as reference media R(■), colored matrix C(■), opalescent matrix T(■), 35 FTU at 11 mPa*s TTV (■), 30 FTU at 20 mPa*s TTVV (■), 16 FTU at 20 mPa*s TVV(■) and clear at 11 mPa*s V(■). See Table 5 for further description of sample matrices. (B) normalized Emission spectra of the individual instruments: blue LED of MFI (■), FlowCam's white LED (■), the 780 nm laser of HIAC and Syringe with 780 nm laser(■) and Syringe with 670 nm laser (■).

Particle Sizing

Although often ignored in practice, common statistical descriptors and tests used in analytical analyses typically require normal distributed data. For the particle counting and sizing studies described below, Skewness and Kurtosis were used to measure departures from normality.[28,29] Skewness and Kurtosis of all populations except "false protein standard" were within acceptable range in order to have minimal error using statistical descriptors and tests (e.g. SD, ANOVA, F-test, t-test) designed for

distributions similar to normal. Therefore “false protein standard” populations could not be statistically analyzed by t- and f-tests for assessing sizing accuracy and precision.

Sizing Accuracy

The population mean particle size values in the various solutions with different physical properties were compared to the mean particle size obtained from the reference suspensions by each of the different individual instruments evaluated. All instruments recognized the 2 µm polystyrene particles as smaller as the nominal values provided by the supplier (Figure 14). Results from the individual methods and solutions differed from one and another. In contrast, the 2 µm borosilicate glass particles in water-like fluid were sized within the range provided in the supplier’s certificate (2.0±0.4µm) for all instruments (Figure 15). The FlowCam instrument shows a very wide distribution compared to other techniques, probably due to the depth of the flow cell leading to particle images being out of focus. Due to this high uncertainty, the effect of the sample matrix seems to play a minor role and can only be seen for matrices with higher refractive indexes (Figure 14). MFI shows very narrow distributions for polystyrene particles, although larger particles (10 µm) are affected by viscosity, and solution population size is lowered by smaller differences in refractive index, respectively. In addition, LO seems to be solely influenced by changes in RI which is not consistent to results comparing HIAC undersizing of 5 µm polystyrene while the Syringe 780 nm recognizes these particles as larger than in water like media (Figure 14). Interestingly, the particles seem to not be affected by turbid or colored sample matrices (Figure 14 and Figure 15). The 8 µm glass spheres are oversized in viscous media using MFI, FlowCam and Syringe 670nm laser whereas the LO instruments with 780nm laser (Syringe 780 and HIAC) show no effect (Figure 15). The emitted wavelength seems to play a role when looking at translucent particles. Most interesting are the findings for the “false protein standard”: practically all LO instruments shifted the populations to smaller size ranges when using media of higher refractive index (Figure 15).

In the second part of this evaluation, the influence of different samples were elucidated by performing a one-tailed t-test with a hypothesized mean difference between two independent populations of zero, i.e. the obtained mean particle size of the respective reference suspension compared to the apparent sizes of the same samples in solutions with different physical properties. The effect sizes (d) for differences from 0.25 µm to 1.25 µm with a step size of 0.5 µm were defined (Table 6) and termed as follows: difference of 0.25 µm is termed "very small", ±0.50 µm "small", ±0.75 µm "medium", ±1.00 µm "large" and ±1.25 µm termed "very large". The effect size (Cohen's d) is defined as the difference between two means divided by a standard deviation for the data. Having different standard deviations the effect sizes for these absolute differences are varying per particle population and instrument used (Table 6). A priori Type I error rate (α), also termed "false positive", was set to 0.05 prior to analysis and power (1-β) was set to 0.80. Keeping α and 1-β constant leads to individual effect sizes (d, Table 6) per particle type and instrument, corresponding individual sample sizes (n_i, Table 7) (which is identical with the number of individual particles) and critical values of a t-distribution (t_{crit}). For each test, the particles of the individual populations were selected by the proportional scaling down of their distributions until the desired sampling size (n_i) was obtained.

Table 6: effect sizes attributed to absolute mean differences between particle populations in reference suspensions and suspensions with …

		Effect size d				
		ΔM= 0.25µm	*ΔM= 0.50µm*	*ΔM= 0.75µm*	*ΔM= 1.00µm*	*ΔM= 1.25µm*
FlowCam 10x	*2µm Polystyrene beads*	0.45	0.90	1.35	1.80	2.25
	5µm Polystyrene beads	0.30	0.60	0.90	1.19	1.49
	10µm Polystyrene beads	0.15	0.31	0.45	0.64	0.76
	2µm glass spheres	0.28	0.56	0.84	1.11	1.39
	8µm glass spheres	0.14	0.29	0.43	0.58	0.72
MFI 5x	*2µm Polystyrene beads*	0.48	0.96	1.44	1.92	2.40
	5µm Polystyrene beads	0.56	1.11	1.67	2.22	2.78
	10µm Polystyrene beads	0.43	0.85	1.28	1.70	2.13
	2µm glass spheres	0.38	0.76	1.14	1.52	1.90
	8µm glass spheres	0.22	0.43	0.65	0.86	1.08
HIAC	*2µm Polystyrene beads*	0.75	1.49	2.24	2.98	3.73
	5µm Polystyrene beads	0.27	0.54	0.81	1.08	1.34
	10µm Polystyrene beads	0.27	0.54	0.81	1.09	1.36
	2µm glass spheres	0.28	0.57	0.85	1.14	1.42
	8µm glass spheres	0.20	0.40	0.59	0.79	0.99
Syringe 670 nm	*2µm Polystyrene beads*	0.48	0.95	1.43	1.91	2.38
	5µm Polystyrene beads	0.71	1.41	2.12	2.83	3.54
	10µm Polystyrene beads	0.65	1.31	1.96	2.61	3.26
	2µm glass spheres	0.29	0.57	0.86	1.15	1.43
	8µm glass spheres	0.24	0.48	0.72	0.96	1.96
Syringe 780 nm	*2µm Polystyrene beads*	0.65	1.30	1.96	2.61	3.26
	5µm Polystyrene beads	0.71	1.43	2.14	2.85	3.56
	10µm Polystyrene beads	0.92	1.83	2.75	3.66	4.58
	2µm glass spheres	0.27	0.55	0.82	1.09	1.37
	8µm glass spheres	0.20	0.40	0.61	0.81	1.01

Table 7: sample sizes (n_i) corresponding to the effect sizes in Table 6.

		sample size n_i				
		ΔM= 0.25µm	*ΔM= 0.50µm*	*ΔM= 0.75µm*	*ΔM= 1.00µm*	*ΔM= 1.25µm*
FlowCam 10x	*2µm Polystyrene beads*	124	32	16	10	8
	5µm Polystyrene beads	280	72	34	20	14
	10µm Polystyrene beads	1086	256	122	62	46
	2µm glass spheres	322	82	38	22	16
	8µm glass spheres	1180	296	134	76	50
MFI 5x	*2µm Polystyrene beads*	110	30	14	10	8
	5µm Polystyrene beads	82	22	12	8	6
	10µm Polystyrene beads	140	36	18	12	8
	2µm glass spheres	174	46	22	14	10
	8µm glass spheres	532	134	62	36	24
HIAC	*2µm Polystyrene beads*	46	14	8	6	5
	5µm Polystyrene beads	342	88	40	24	16
	10µm Polystyrene beads	338	86	40	24	16
	2µm glass spheres	310	80	36	22	14
	8µm glass spheres	632	160	72	42	28
Syringe 670 nm	*2µm Polystyrene beads*	112	30	14	10	8
	5µm Polystyrene beads	52	14	8	7	6
	10µm Polystyrene beads	60	18	10	7	6
	2µm glass spheres	304	78	36	22	14
	8µm glass spheres	434	110	50	30	10
Syringe 780 nm	*2µm Polystyrene beads*	60	18	10	6	5
	5µm Polystyrene beads	52	14	8	7	6
	10µm Polystyrene beads	32	10	6	5	4
	2µm glass spheres	332	84	40	24	16
	8µm glass spheres	608	154	70	40	26

Generally, there were only minor sizing effects observed with polystyrene particle bead standards in the different solutions as measured by the different instruments (Table 9 and Figure 14). More differences in sizing effects were seen when evaluating translucent glass particles (Table 9, Table 8 and Figure 15). This result is probably due to the fact that most of the interaction with light is adsorption and reflection for polystyrene particles. The fraction of light being refracted is larger for glass particles and therefore changes in refraction index influenced the particle sizing.

With regards to the 8µm glass spheres, LO by HIAC (HIA) was underestimating particle size values in viscous media, whereas all other methods showed either only marginal effects (e.g., Syringe with 780nm laser, SY7) or recognized the particles as larger when decreasing the difference of refractive index. HIAC maeasurements also underestimated 5 and 10µm polystyrene particles with increasing solution viscosity, as well as decreasing refractive index of media and particles, respectively (Table 9 and Figure 14).

Given that the 2 µm particles are at the very edge of detection (for MDI and LO methodologies due to Abbe Limit), one can observe the appearance of airy discs that is significantly changing with decreasing differences in refractive index (Table 8). As these analytical systems are typically calibrated using particles that highly differ in refractive index from the fluid – namely polystyrene in water – this effect is likely leading to large sizing effects. The effect is rather marginal, however, when varying the emitting wavelength of the instrument (LO with 670nm Laser (SY6) vs. LO with 780nm laser (SY7)).

Table 8: Visualization of calculated differences in refraction and diffraction properties for translucent glass particles in water (R) and a glycerol/water mixture (V). See Table 5 for further description of sample matrices.

Matrix	refraction for 8 µm glass sphere	Diffraction for a 2 µm glas sphere at 780 nm (airy discs)
R	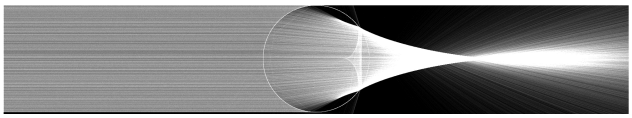	
V	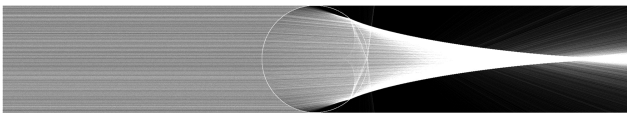	

MDI methods did not show large variations in sizing except for MFI 8, 10 µm glass particles which were recognized as 0.7 µm smaller than in the reference suspension (Table 9 and Figure 15).

LO methods showed large variations in sizing (0.3-0.5 µm difference) for 5 and 10 µm polystyrene bead particles whereas solution viscosity caused the most significant difference. However, this finding could not be well-correlated to the decrease in difference in refractive index of solution or particles, for example, glass particles with a $R_i = 1.56$ were less affected than polystyrene particles ($R_i = 1.59$). In addition, the matrices containing more glycerol did not largely differ in refractive index (Table 9 and Figure 14).

The effect of solution viscosity on MFI measurements of small glass particles was observed and is likely attributed to the refractive index. Small differences in sizing were observed for all particle types and particle sizes except for 2 µm glass particles recognized by instruments having a 780 nm laser. These sizing differences, however, were marginal (Table 9 and Figure 15) and potentially not of practical relevance. In contrast to reports in literature, no medium effects or large differences in particle sizing were observed for LO methods analyzing glass beads in viscous media, and media of similar refractive index, respectively.[30]

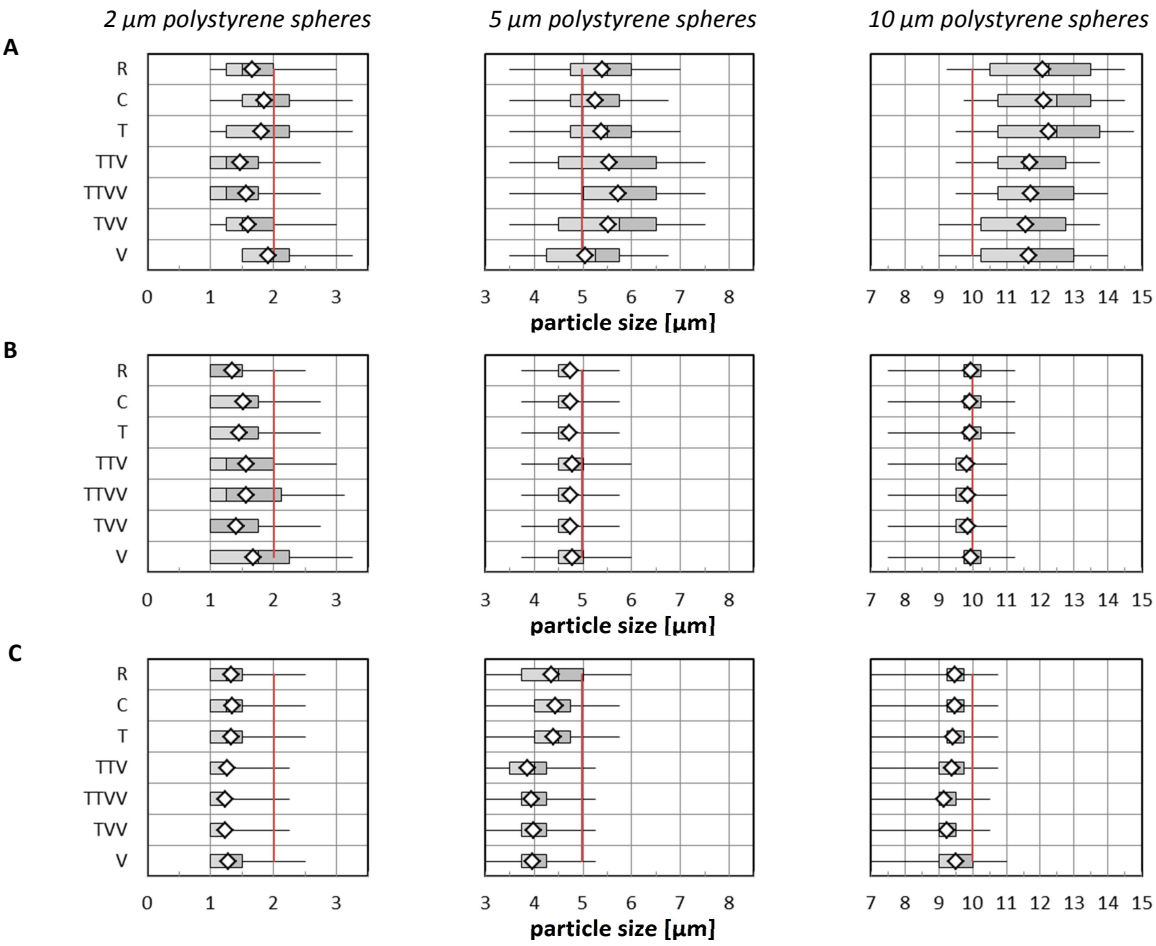
2 µm polystyrene spheres
5 µm polystyrene spheres
10 µm polystyrene spheres
A
B
C
R
C
T
TTV
TTVV
TVV
V
0 1 2 3
3 4 5 6 7 8
7 8 9 10 11 12 13 14 15
particle size [µm]

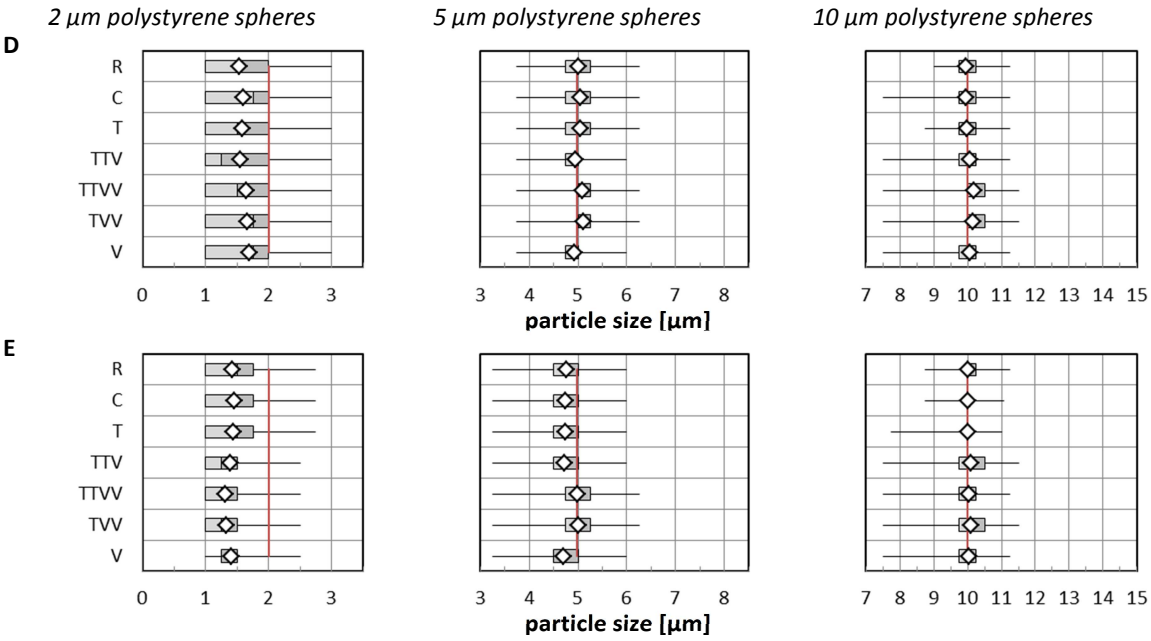

Figure 14: Particle size analysis of polystyrene bead standards in solutions with different physical properties as measured by A) FLowCam, B) MFI, C) HIAC, D) Syringe with 670 nm Laser and E) Syringe with 780 nm Laser. Samples include water reference(R), colored matrix (C), opalescent matrix with 50 FTU (T), 35 FTU at 11 mPa*s (TTV), 30 FTU at 20m Pa*s (TTVV), 16 FTU at 20mPa*s (TVV) and clear at 11m Pa*s (V). Analysis of particle populations presented by box-plot with n=10000 per boxplot. The left whisker points to the population's minimum (min) whereas the right whisker shows its maximum (max) value. The box represents the middle 50% of the population whereas it is vertically broken by a black line at the population's median (Mdn). The marker represents the populations mean (M). The vertical red line represents the particle population's mean size value according to supplier's information.

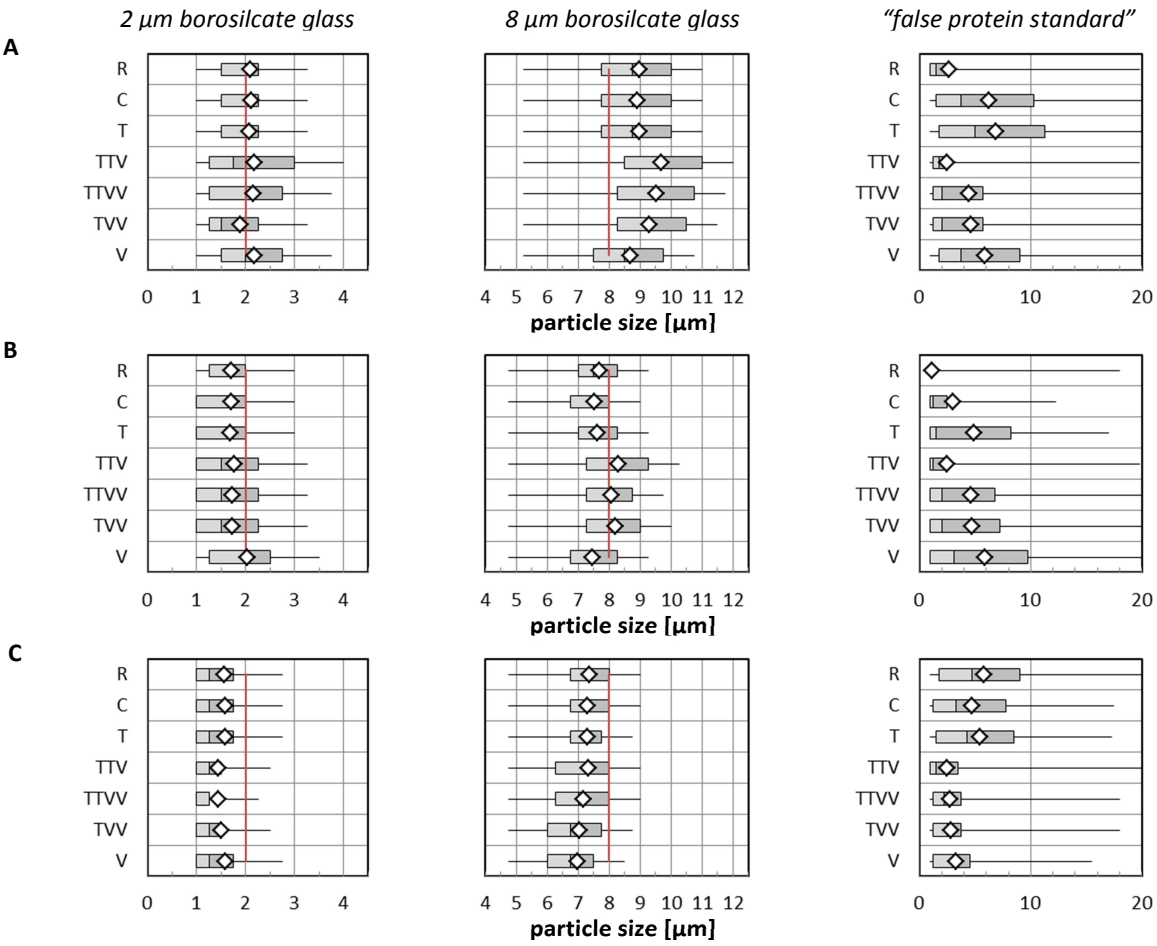
A
B
C
2 µm borosilcate glass
8 µm borosilcate glass
"false protein standard"
R
C
T
TTV
TTVV
TVV
V
0 1 2 3 4
4 5 6 7 8 9 10 11 12
0 10 20
particle size [µm]

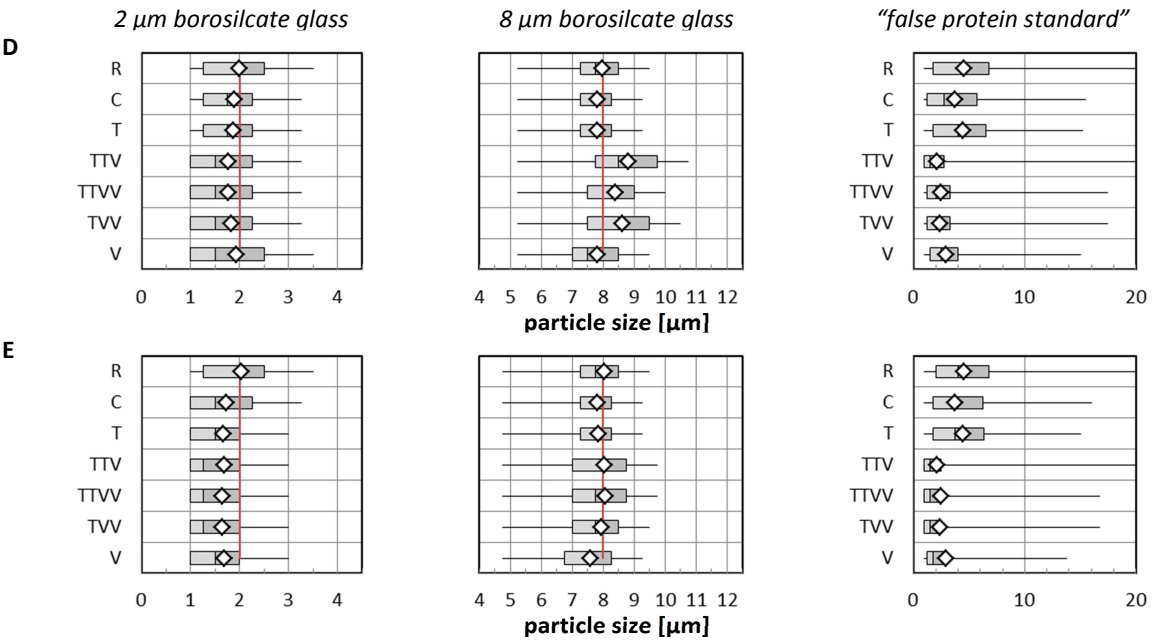

Figure 15: Particle size analysis of glass bead standards and a false protein standard in solutions as measured by A) FLowCam, B) MFI, C) HIAC, D) Syringe with 670nm Laser and E) Syringe with 780nm Laser. Samples include water based reference (R), colored matrix (C), opalescent matrix with 50 FTU (T), 35 FTU at 11 mPa*s (TTV), 30 FTU at 20 mPa*s (TTVV), 16 FTU at 20 mPa*s (TVV) and clear at 11 mPa*s (V). Analysis of particle populations presented by box-plot with n=10000 per boxplot. The left whisker points to the population's minimum (min) whereas the right whisker shows its maximum (max) value. The box represents the middle 50% of the population whereas it is vertically broken by a black line at the population's median (Mdn). The marker represents the populations mean (M). The vertical red line represents the population's mean of according to supplier's information.

Table 9: The statistical significance of measured particle populations in different solution matrices was addressed using the one sided t-test with a hypothesized mean difference of zero as a function of different particle sizes. Values in table show the smallest sizing effect which was significant for different solution matrices in comparison to the water-reference standard. Differences with respective to the water-reference suspensions (R) are shown for each sample matrix as a function of particle size in µm (values greater zero show a significant shift to larger particle sizes, negative values to smaller sizes, zeros represent no significant difference color code: -1.25µm ±0.00µm +1.25µm). See Table 5 for further description of sample matrices.

Method	Sample Matrix	Polystyrene particles			Borosilicate glass spheres	
		2µm	5µm	10µm	2µm	8µm
FLO	*C*	0.25	-0.25	0	0	0
	T	0.25	0	0.25	0	0
	TTV	-0.25	0	-0.25	0	1.25
	TTVV	0	1.25	-0.25	0	1.25
	TVV	0	0	-1.25	-0.75	0.25
	V	0.75	-0.25	-0.75	0	0.25
MFI	*C*	0.75	0	0	0	0
	T	0	0	0	0	0
	TTV	0	0	0	0	1
	TTVV	0.25	0	0	0	0.75
	TVV	0	0	0	0	0.75
	V	0.75	0	0	0.25	-0.25
HIA	*C*	0	0	0	0	0
	T	0	0	0	0	0
	TTV	0	-0.75	0	0	0
	TTVV	0	-0.75	-1.25	0	-0.25
	TVV	0	-1.25	-1.25	0	-1.25
	V	0	-0.75	0	0	-1
SY6	*C*	0	0	0	0	0
	T	0	0	0	0	-0.25
	TTV	0	0	0	-0.25	0.75
	TTVV	0	0	0.25	-0.25	0.75
	TVV	0	0	0.25	0	0.75
	V	1.25	-0.25	0	0	-0.25
SY7	*C*	0	0	0	-0.75	-0.25
	T	0	0	0	-0.75	-0.25
	TTV	0	0	0	-0.75	0
	TTVV	-0.25	0.25	0	-0.75	0
	TVV	-0.25	0.25	0	-0.75	0
	V	0	0	0	-0.75	-0.75

Sizing Precision

In terms of sizing precision, a coefficient of variance which is only attributed to the individual instruments response was applied. This CV_i is defined as the square root of the difference of the observed sizing variance (sd_{obs}^2) and the particle variance reported by the supplier (sd_p^2) divided by the particle diameter (D_p) as certified by the supplier.[31,32] Within context of the USP <788> and EP pharmacopeia tests, this index is solely attributed to the instruments response and also termed "sensor resolution".[1-3]

Equation 3: coefficient of variance attributed to instruments response ("sensor resolution")

$$CV_i = \frac{\sqrt{sd_{obs}^2 - sd_p^2}}{D_p}$$

In order to pass the test for sensor resolution according to EP and USP, the CV_i has to be lower than 0.1 for narrowly distributed, well-defined particles such as 10 µm polystyrene particle size standards. LO instruments with a noise level meeting the <0.1 resolution requirement are also stated as showing acceptable counting agreement.[26]

An overview of the obtained sensor resolutions is shown in Figure 16 and Figure 17 for MDI and LO methods, respectively. In general, the resolution of 2 µm particles was low. This observation was potentially due to the diffraction in LO sensors and the small pixel number and brightness in MDI sensors.

For the FlowCam (FLO) instrument, sensor resolution was in general low and decreased up to 53% for 2 µm glass particles when using solution matrices with combined turbid and viscous properties (Figure 16). Sensor resolution did not change significantly using MFI and polystyrene particles (except for 2 µm polystyrene beads), but showed significant decrease for 2 µm glass particles (up to 30% lower resolution for refractive indices of 1.42, 1.43 respectively). In contrast, the effect of lowering the sensor

resolution on results from the LO methods (especially for the 670 nm sensor) was rather marginal for larger particles, but more significant for the smaller 2 µm populations (Figure 17).

For the LO methods, the syringe sensors instrument showed a better resolution compared to the HIAC/Royco (HIA), and precision results stayed below 10% for 10 µm polystyrene standards as shown in Figure 17. With regards to glass particles, the 670 nm laser (SY6) showed marginally better results for reference suspensions whereas the 780 nm laser (SY7) was less influenced by the sample fluid when evaluating glass particle suspensions. The balancing of these pro and cons is required for a decision in terms of selecting one of the two laser wavelengths for measuring particle sizes by a LO method.

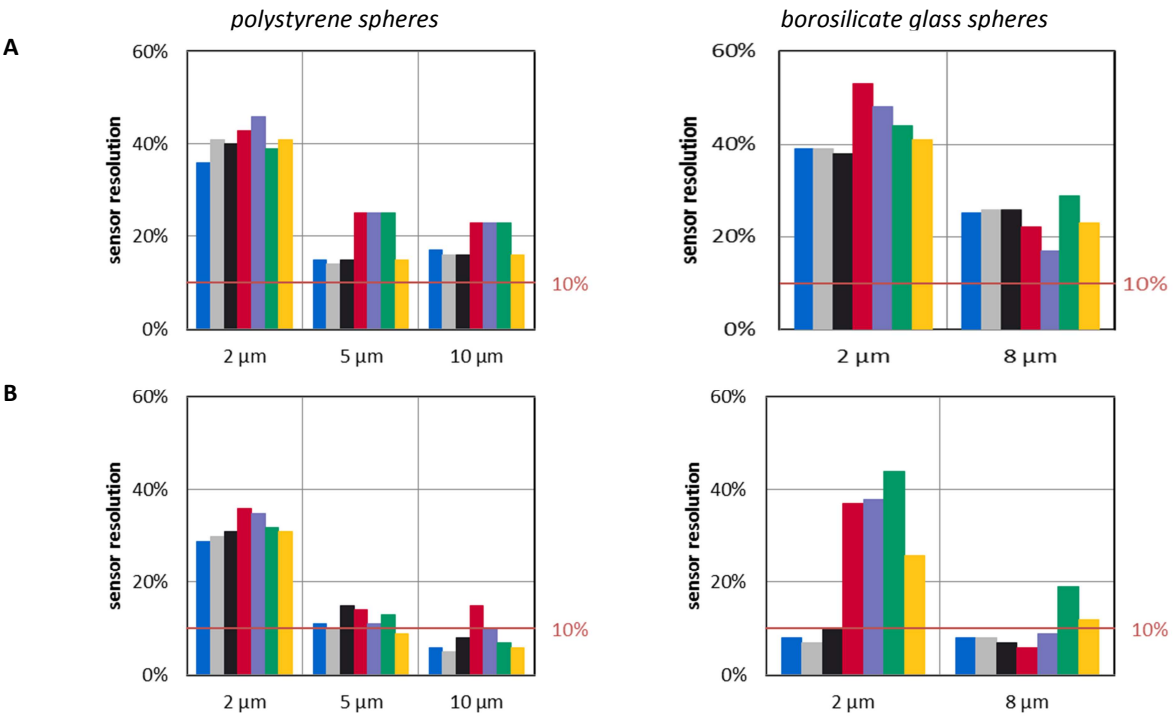

Figure 16: Sensor resolution for polystyrene and borosilicate glass particle bead standards in different solutions using different MDI instruments: (A) FlowCam (FLO), (B) MFI dpa4200 (MFI). Samples matrcies include water as reference media R(■), colored matrix C(■), opalescent matrix T(■), 35 FTU at 11 mPa*s TTV (■), 30 FTU at 20 mPa*s TTVV (■), 16 FTU at 20 mPa*s TVV(■) and clear at 11 mPa*s V(■).The horizontal red lines represent 10% sensor resolution. See Table 5 for further description of sample matrices.

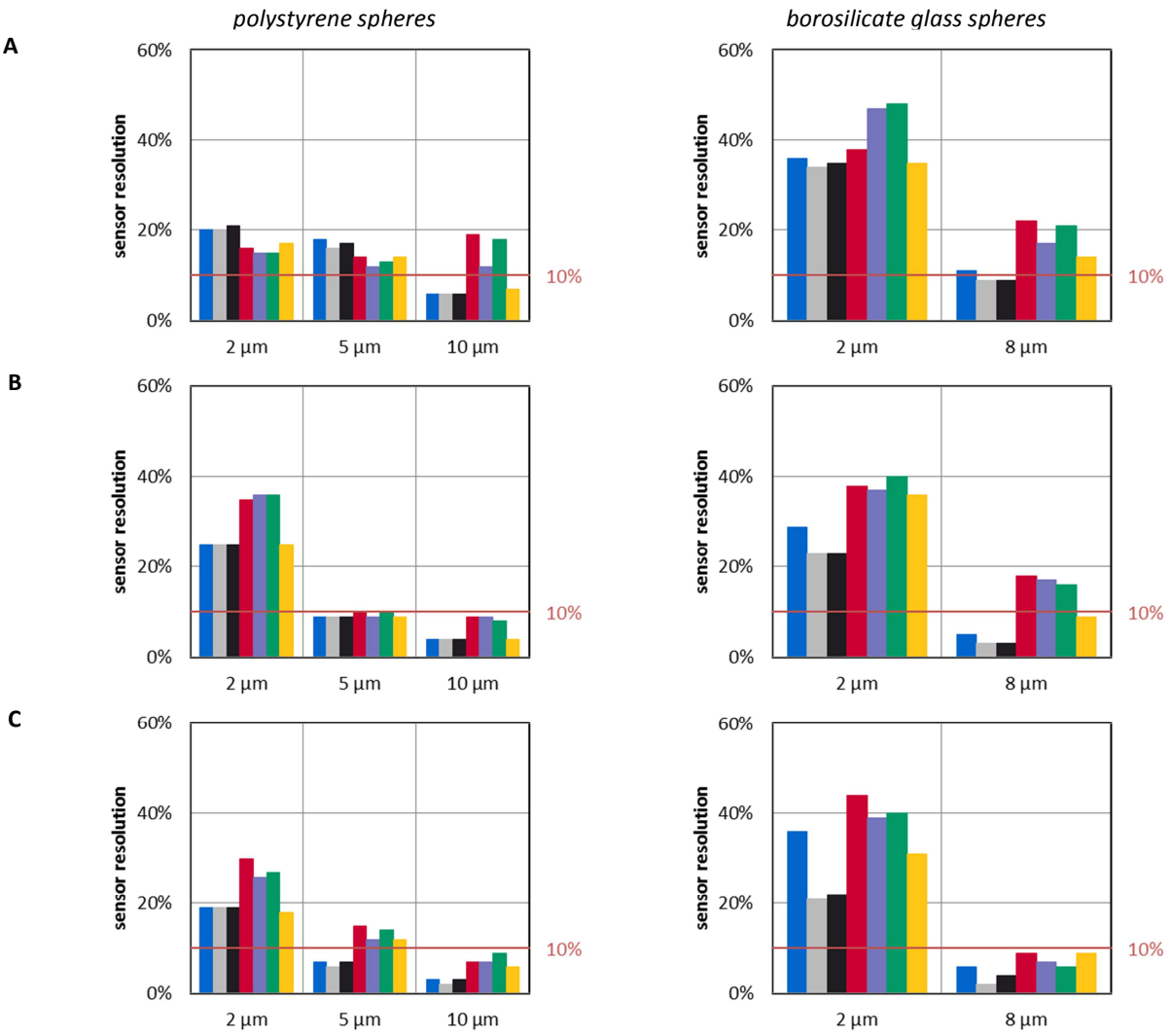

Figure 17: Sensor resolution for polystyrene and borosilicate glass particle bead standards in different solutions using different LO instruments: (A) HIAC (HIA), (B) Syringe with 670 nm laser (SY6), (C) Syringe with 780 nm laser (SY7). Sample matrices included water as reference media R(■), colored matrix C(■), opalescent matrix T(■), 35 FTU at 11 mPa*s TTV (■), 30 FTU at 20 mPa*s TTVV (■), 16 FTU at 20 mPa*s TVV(■) and clear at 11 mPa*s V(■).The horizontal red lines represent 10% sensor resolution. See Table 5 for further description of sample matrices.

Counting Ability

Counting Accuracy

For each instrument and individual particle samples in different solutions, four independent repetitions were performed. Special attention was given to sample handling and homogenization in order to obtain reliable and reproducible results. Prior to analysis, each sample was gently inverted 20 times. During these experiments, sinking velocity was observed during pre-tests (data not shown) with large glass particles resulting in not being able to these particles. Contamination was minimized by working in clean environments and by opening sample containers only at the time of sample injection. It should be pointed out, however, for a statistical evaluation with sufficiently high power and error probabilities, more repetitions per sample would be needed. The following results are therefore presented conventionally and the conclusions drawn should be more seen as indicating trends and correlations.

A couple of additional comments are warranted prior to presenting the data in Figures 18, 19, and 20. First, the LO methods using reference suspensions showed higher counts for glass particles. This was attributed to low flow speed in MDI methods and high sink velocities of glass particles. The reference counts in LO are therefore considered more reliable and also closer to the expected values (Figure 18). Second, the particle counts for polystyrene and glass particles shown below (Figure 19 and Figure 20, 1st and 2nd column) are reported as greater or equal to a specified particle size when particle counting efficiency reaches 100%. Third, due the actual size distribution for the "False Protein Standard", which is much broader than the particle sensors range, particle counts for sizes ≥ 2 µm, ≥ 5 µm, ≥ 10 µm and ≥ 25 µm are reported (Figure 19, 3rd column). The first of these particle size ranges is at the very limit of the sensor, and are reported for information only, whereas the latter two size channels are required by EP and USP.[1-3]

With regard to the polystyrene reference suspensions (Figure 18A), the FlowCam method showed higher particle counts for all of the polystyrene bead particle sizes examined, whereas the MFI, Syringe 670nm (SY6) and Syringe 780nm (SY7) instruments were within the expected range. Interestingly, HIAC particle counts for 5 and 10 µm polystyrene particles were less than the calculated values. Although the 2 µm glass particles (Figure 18B) were recognized by the LO methods, the observed particle counts did not correspond well to the calculated level. This lack of recognition could be attributed to the particle's translucence combined with the relatively broad size distribution of the glass particles. The translucence of the particle would lead to an underestimation of particle size, and consequently, part of the particle distribution might not be not recognized accurately. The expected 2, 8 and 10 µm glass particle counts by the MDI methods were also not achieved, which is potentially due to the slow flow speed and the high density of the glass particles. In terms of analyzing the "false protein standards" (Figure 18C), MDI showed significantly higher particle counts than the LO methods for smaller size ranges, which is potentially due to fragmentation artifacts of larger particles and/or potentially inhomogeneous sample illumination. There were less counting differences observed for larger particles between MDI and LO. These discrepancies can be attributed to their high translucence and/or the slight underestimation of MDI methods if digital fragmentation on larger particles occurs.

Figure 19 and Figure 20 show counting accuracy for MFI and LO instruments, respectively. Colored or turbid suspensions did not significantly affect counting of polystyrene or glass particles (Figure 19 and Figure 20). The influence of viscous suspensions and combinations of turbid and viscous suspensions to the counting accuracy was, however, significant yet it did not consistently follow a simple relationship: e.g., the FlowCam showed higher counts for glass and polystyrene particles (especially for smaller particles not larger than 5 µm) in solutions with 35FTU at 11mPa*s and 16 FTU at 20 mPa*s, but not in solutions with 30 FTU at 20mPa*s or clear solutions at 11mPa*s (Figure 19). MFI measurements

simply counted less particles when the difference in refractive index of particles and solutions was decreased (Figure 19).

Similar to FlowCam, the HIAC method showed significantly more particles in solutions with 35FTU at 11mPa*s and 16 FTU at 20 mPa*s for all tested particles (Figure 20 and Figure 19). The Syringe 670nm was comparable to the Syringe 780nm when measuring polystyrene particles, but showed higher counts for glass beads and “false protein standard” (Figure 20). This result of higher sensitivity for measuring translucent particles using a smaller emission wavelength LO instrument is consistent with results observed with the FlowCam (white LED) and MFI (blue LED) instruments. Yet LO instrument was more affected by the refractive index of the sample matrix with regards to precision being less robust (Figure 20). Thus, a lower wavelength instrument seems to be more sensitive to measuring the size of translucent particles, and therefore, instrument design and detector type both likely play a major role in terms of particle counting as we can see when comparing HIAC, Syringe 670 and Syringe 780 (Figure 20).

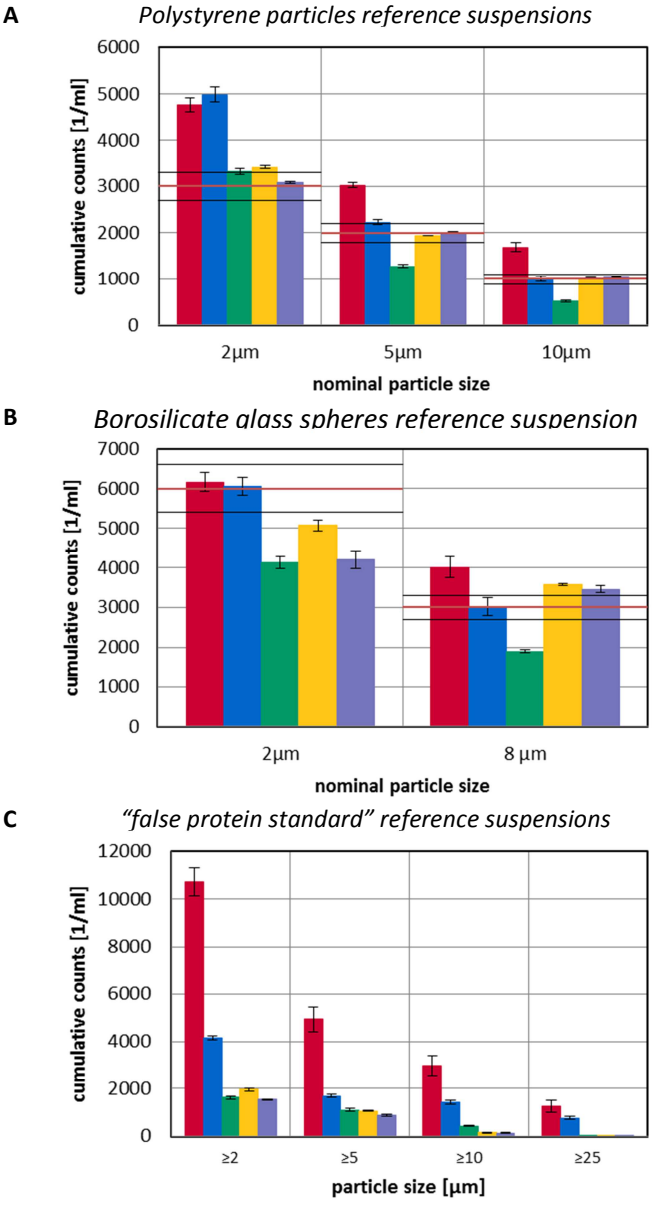

Figure 18: Particle counts of reference suspensions of (A) polystyrene particles, (B) borosilicate glass spheres, and (C) "false protein standard" using MDI including FlowCam (■), MFI (■), and LO including HIAC(■), Syringe 670 nm laser (■) and Syringe 780 nm laser (■). The horizontal red lines in A and B represent the calculated values and the black horizontal lines are ±10% of the expected value. The error bars represent ±sd of n=4 independent measurements.

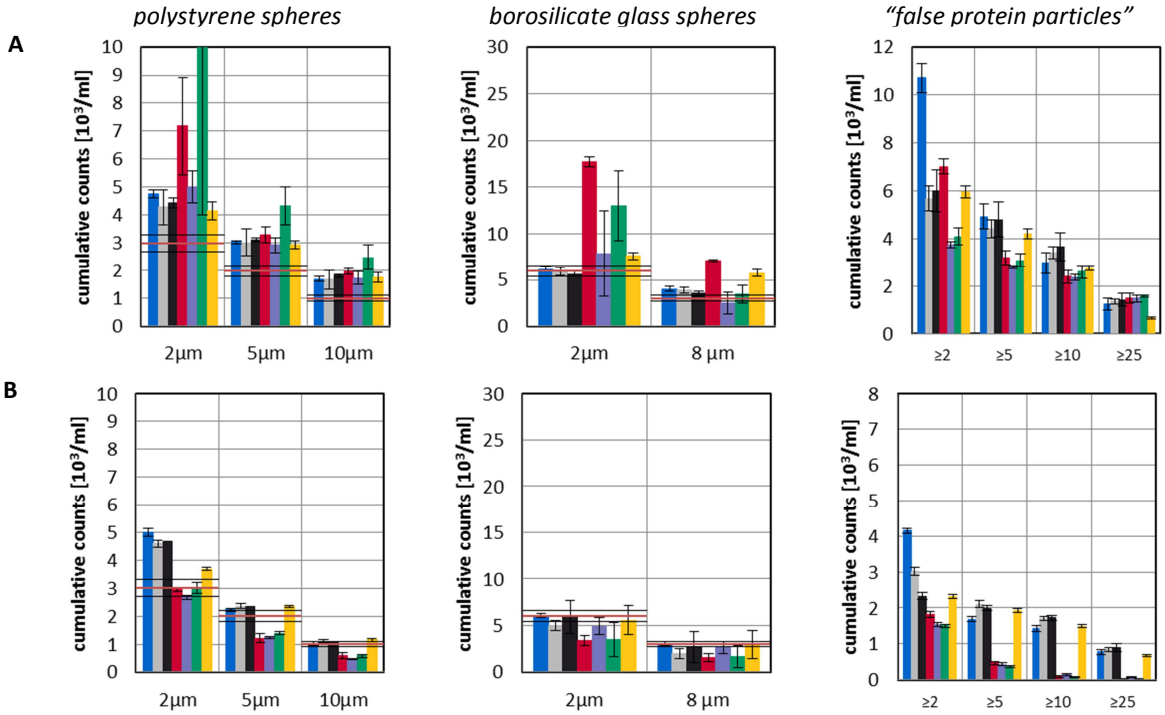

Figure 19: Particle counts for polystyrene particle bead standards (1st column), borosilicate glass particle bead standards (2nd column) and “false protein standards” (3rd column) using MDI instruments (A) FlowCam, and (B) MFI. Particle standards were suspended in water as reference media R(■), colored matrix C(■), opalescent matrix T(■), 35 FTU at 11 mPa*s TTV (■), 30 FTU at 20 mPa*s TTVV (■), 16 FTU at 20 mPa*s TVV(■) and clear at 11 mPa*s V(■).The horizontal red lines represent 10% sensor resolution. See Table 5 for further description of sample matrices. The horizontal red lines represent the calculated values and the black horizontal lines are ±10% of the expected value. The error bars represent ±sd of n=4 independent measurements.

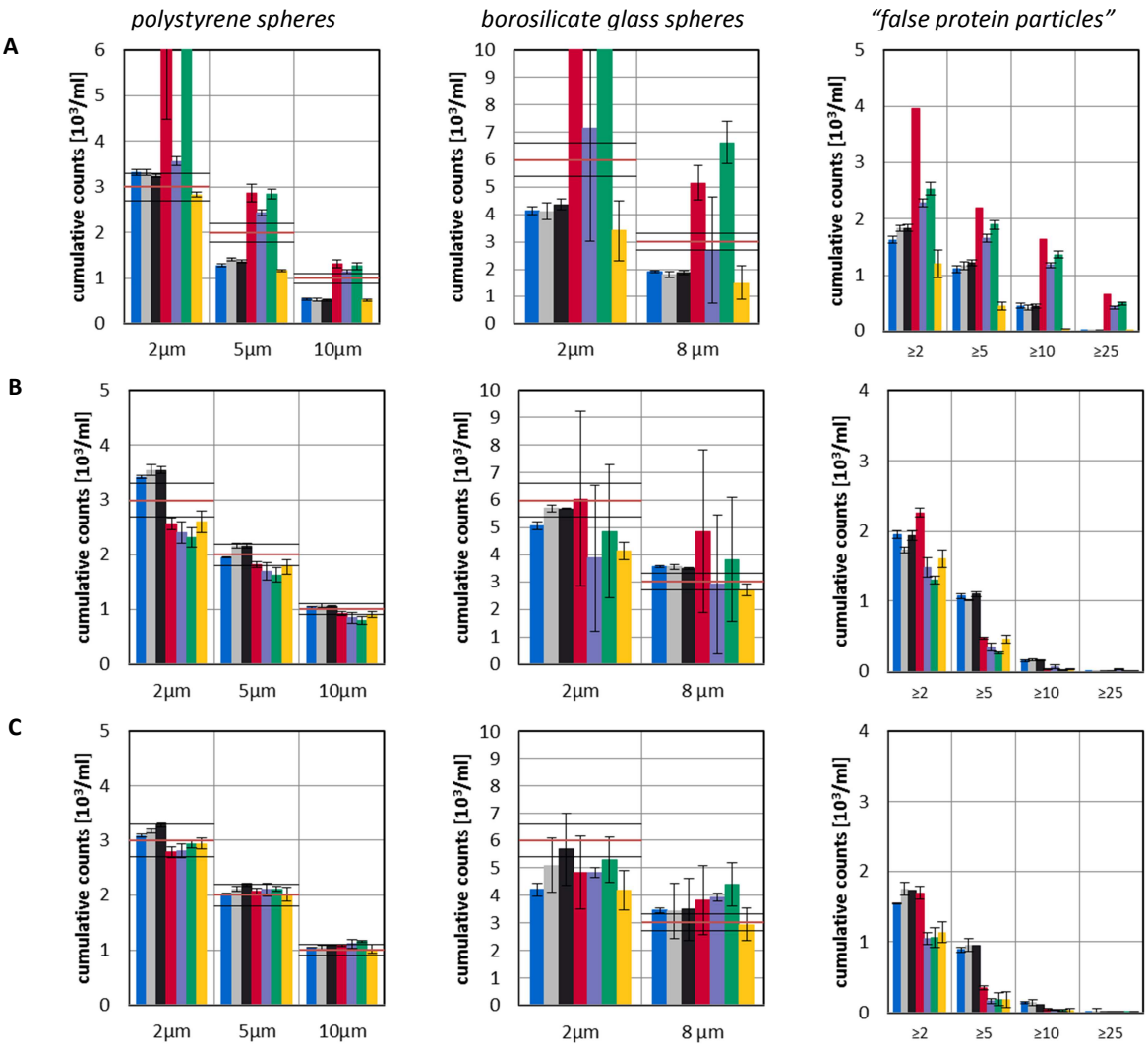

Figure 20: Particle counts for polystyrene bead standard particles (1st column), borosilicate glass bead standard particles (2nd column) and "false protein standards" (3rd column) using LO instruments (A) HIAC, (B) Syringe 670 nm, and (C) Syringe 780 nm. Particle standards were suspended in water as reference media R(■), colored matrix C(■), opalescent matrix T(■), 35 FTU at 11 mPa*s TTV (■), 30 FTU at 20 mPa*s TTVV (■), 16 FTU at 20 mPa*s TVV(■) and clear at 11 mPa*s V(■).The horizontal red lines represent 10% sensor resolution. See Table 5 for further description of sample matrices. The horizontal red lines represent the calculated values and the black horizontal lines are ±10% of the expected value. The error bars represent ±sd of n=4 independent measurements.

Counting Precision

As a characteristic parameter for determining particle counting precision, coefficients of variances (CV) were used which were calculated by dividing the standard deviation (sd) of n=4 particle count measurements obtained for a certain particle size range divided by the particle count average obtained for that size. The particle sizes examined in this study were equal to the sizes used in the previous section on particle counting accuracy.

Equation 4: coefficient of variance for counting precision

$$CV_i = \frac{sd_i}{M_i}$$

When elucidating counting precision of measurements with polystyrene and glass particle bead standards (Figure 21), all methods showed repeatable results for the reference suspensions. A number of interesting relations are shown in Figure 21. However, these results have to be examined carefully due the small number of experiments and only few of the observations were considered to be of practical relevance as discussed below.

As expected, counting reproducibility for glass particles was more affected by different solution properties than polystyrene particles. Solution turbidity and viscosity showed similar effects of lowering reproducibility. Counting precision using LO methods was less affected than MDI methods for measuring glass particles, which again may be attributed to the higher density of the glass particles, and therefore, a higher sink velocity. Using the “false protein standards”, counting reproducibility was 10% lower for MDI methods. LO methods showed slightly better reproducibility which decreased at higher particle size ranges, especially for counts ≥10 µm, however, one has to keep in mind that the LO method was only detecting a few particles at the higher size ranges.

Interestingly, suspensions containing colored solutions with glass particles were challenging in terms of FlowCam (FLO) and MFI reproducibility. In terms of solution viscosity, one could assume that the higher variability of particle counts at increased sample viscosity would most likely be due to potential air bubble formation during sample homogenization. However, in this set of experiments, air bubbles were not observed for high viscosity samples and therefore particle counts did not noticeably increase. Lower reproducibility is not fully understood at this time, but may partially be attributed to homogenization problems due to difference in diffusion coefficients.

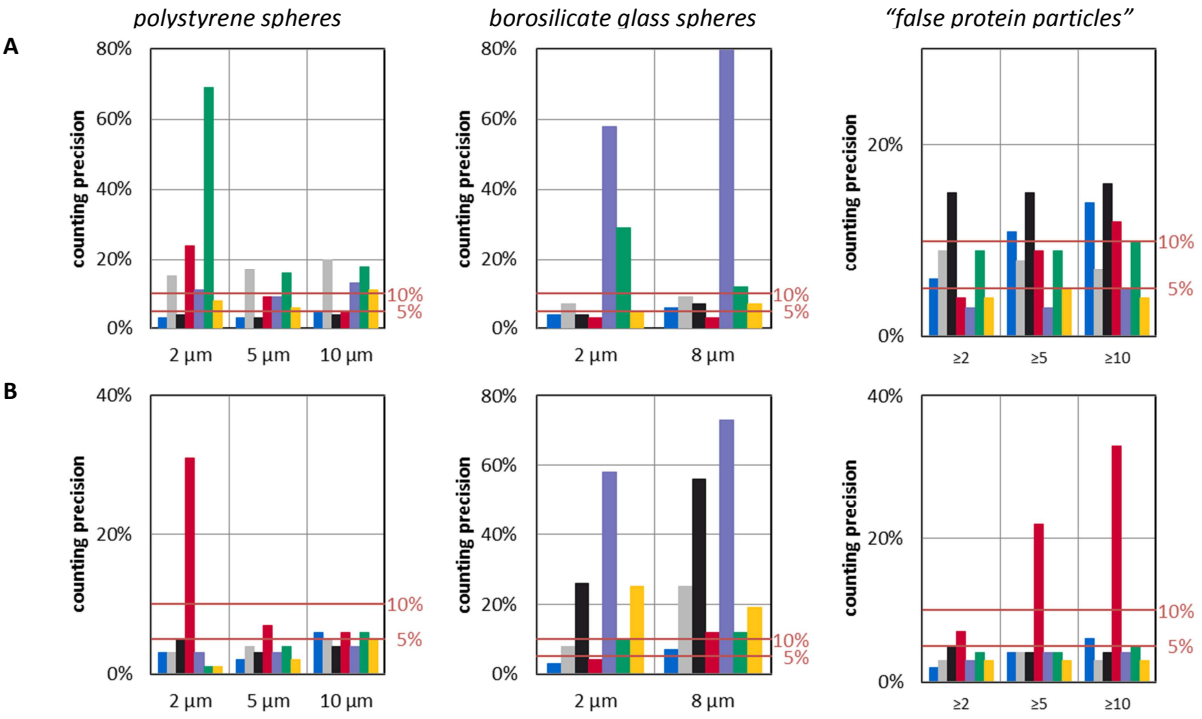

Figure 21: Particle counting precision of n=4 independent measurements with MDI instruments (A) FlowCam (FLO), (B) MFI, for different particle standards suspended in water as reference media R(■), colored matrix C(■), opalescent matrix T(■), 35 FTU at 11 mPa*s TTV (■), 30 FTU at 20 mPa*s TTVV (■), 16 FTU at 20 mPa*s TVV(■) and clear at 11 mPa*s V(■).The horizontal red lines represent 10% sensor resolution. See Table 5 for further description of sample matrices.

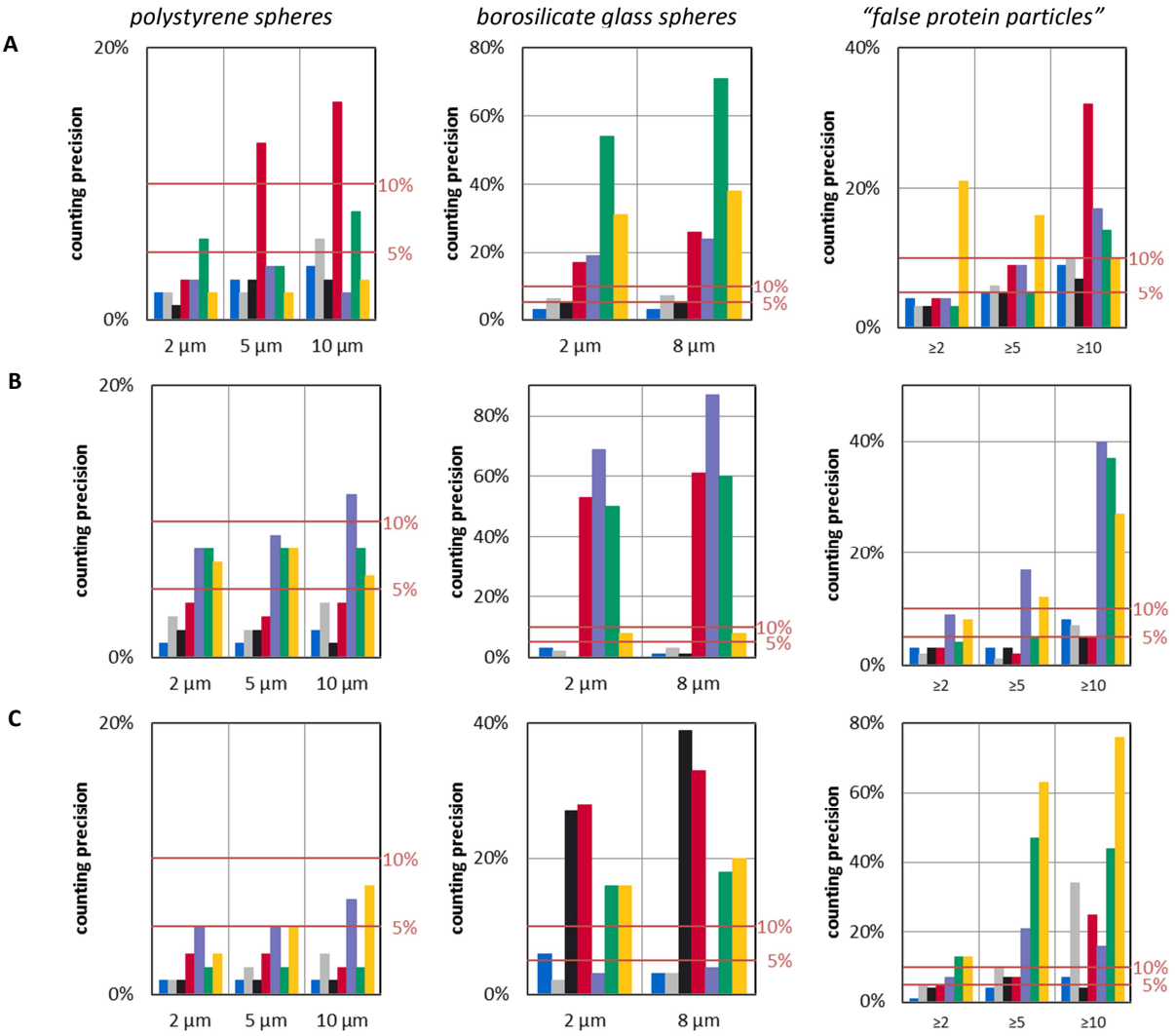

Figure 22: Particle counting precision of n=4 independent measurements with LO instruments (A) HIAC, (B) Syringe with 670 nm laser (SY6), and (C) Syringe with 780 nm laser (SY7). Different particle standards were suspended in water as reference media R(■), colored matrix C(■), opalescent matrix T(■), 35 FTU at 11 mPa*s TTV (■), 30 FTU at 20 mPa*s TTVV (■), 16 FTU at 20 mPa*s TVV(■) and clear at 11 mPa*s V(■).The horizontal red lines represent 10% sensor resolution. See Table 5 for further description of sample matrices.

Conclusions

A small sample volume LO method was verified and compared to the larger volume USP/EP LO method for counting a variety of subvisible particles including polystyrene beads and aged mAb samples. Comparisons of LO and MDI methods were then carried out to determine the advantages and limitations for each analytical technique. Small sample LO and MFI resulted in differences in particle counts, however, these differences could not solely be attributed to the irregular shape and/or translucency of proteinaceous particles. For instance, MFI 5x counts for particles < 3 µm were significantly higher than for MFI 14x counts for the different particle types analyzed. Thus, MFI 5x particle counts at the lower particle size range should be verified with an alternative method, e.g. MFI 14x. However, the MFI 14x method is lacking in terms of key parameters such as sampling efficiency and sufficient sample throughput. Though potential artifacts in MDI measurements may lead to higher particle counts in the 2 µm range, the reasons for the differences of MDI and LO measurements are still not fully understood and were further elucidated in subsequent studies. In contrast to previous publications, differentiation of particle types by shape analysis (mean intensity and circularity) using MFI was only possible for larger particles.[7] Furthermore, differentiation of particle types based only on one shape parameter and using absolute data analysis filters remains challenging. A reliable differentiation of particles was only possible for particles > 5 µm or even > 10 µm and depended on factors such as their similarity, the chosen shape parameter, and the instrument type. For smaller particles, differences in shape parameters for various particle types could not be observed using MFI. In summary, flow imaging techniques are helpful for characterization of the shape and morphology of sub-visible particles, but comparison of sub-visible particle counts and quantities between methods should be taken with care. In terms of particle shape analysis, picture quality is a key parameter when comparing different instruments.

A performance overview for the influence of sample fluid to counting and sizing abilities is given in Table 10 and Table 11. A number of conclusions can be drawn from these experiments studying the effect of variations of the sample matrix on particle counting, but only a few are considered to be the most relevant for practical applications: FlowCam showed low sizing and counting abilities compared to all other methods tested, most likely due to limitations in sampling efficiency and depth of the flow cell. Nevertheless, it was capable of recording higher quality particle pictures which can potentially better help to identify the particle origin. MFI images were sharper and more precise in terms of counting and sizing, but their picture quality appears lower due to lower pixel density per micron which is directly attributed to the magnification and the digital sensor (lower magnification) of the MFI. All of the instruments achieved the required sizing resolution testing according to USP<788> with the exception of the FlowCam instrument. Based on these results, LO remains the gold standard for the quantification of sub-visible particles in a QC environment, but MFI capabilities have greatly improved during the last few years and may in future also provide counting and sizing capabilities for QC use. Currently, MFI still lacks LO in terms of sample efficiency and sample throughput.

The effect of physical properties of sample matrices on the accuracy and precision of particle counting and sizing was examined in detail. The coloration and turbidity of a solution had only a relatively small effect on particle sizing and counting ability. However, whereas counting precision with the Syringe 780 nm and MFI instruments was significantly lower for 8 µm glass particle measurements in turbid media, particle sizing was not affected. The viscosity of a solution showed a pronounced influence on particle results, especially when using translucent glass particles or a non-uniform “false protein standard”. High viscosity samples may contribute to inaccurate particle counts due to air bubble formation, although air bubbles were not definitively imaged by MFI or FlowCam in this series of experiments. Viscosity also affects particle sizing accuracy for the HIAC method, especially when evaluating 5 or 10 µm polystyrene particles or 2 µm glass particles.

Viscosity mostly affected counting reproducibility; yet, only 4 independent measurements have been performed in the course of this study. Counting precision was most affected when testing the borosilicate glass bead standards using MFI or Syringe 670 nm instruments.

Polystyrene standards are considered very robust against effects of sample matrix solution properties differing from water, and therefore are still considered the best option to calibrate these SbVP instruments. Nonetheless, new particle standards that better resemble protein particles, with well-defined shapes and monodisperse sizes, would be very beneficial to quantitatively assess and understand the limitations of each of the analytical instruments. However, the reproducible generation and long term stability of these protein based particle standards remains a significant challenge. In summary, despite the availability of new MDI instruments, the detection and counting sub-visible protein based particles, especially particles of larger or equal than 2 µm, remains challenging, especially in a QC environment, depending on the instrument used, the solution properties, and the size and shape of the particles.

Table 10: performance overview of sample matrix influence for polystyrene particles standards suspended in water as reference media (R), colored matrix (C), opalescent matrix (T), 35 FTU at 11 mPa*s (TTV), 30 FTU at 20 mPa*s (TTVV), 16 FTU at 20 mPa*s (TVV) and clear at 11 mPa*s (V). For the individual samples following key parameters are shown: counting accuracy: the difference between the observed particle size (n=10000) and the suppliers certified size in µm ($\Delta M_{ø}$); sizing precision: the sensor resolution according to EP/USP in % ($CV_{ø}$); counting accuracy: the difference between the calculated value and the observed mean particle counts (n=4) in particles per ml ($\Delta M_{\#}$); counting precision the standard deviation devided by the mean particle counts n=4 individual measurements in % (CV#). The individual columns are colored in gradient from low to high performance (BAD NEUTRAL GOOD)

		Polystyrene particles											
		2µm				5µm				10µm			
		$\Delta M_{ø}$	$CV_{ø}$	$\Delta M_{\#}$	$CV_{\#}$	$\Delta M_{ø}$	$CV_{ø}$	$\Delta M_{\#}$	$CV_{\#}$	$\Delta M_{ø}$	$CV_{ø}$	$\Delta M_{\#}$	$CV_{\#}$
FloCam 10x	R	0.3	28%	586	3%	0.4	17%	515	2%	2.1	17%	697	5%
	C	0.2	29%	427	15%	0.3	16%	508	16%	2.1	16%	681	20%
	T	0.2	28%	480	4%	0.4	17%	562	3%	2.3	16%	815	4%
	TTV	0.5	28%	1396	24%	0.6	25%	642	9%	1.7	20%	962	5%
	TTVV	0.4	30%	673	11%	0.7	22%	465	9%	1.7	19%	733	13%
	TVV	0.4	27%	3267	69%	0.5	25%	1162	16%	1.6	19%	1493	18%
	V	0.1	28%	387	8%	0.1	17%	473	5%	1.7	16%	752	11%
MFI 5x	R	0.7	26%	663	3%	0.2	9%	116	2%	0.0	6%	12	6%
	C	0.5	27%	530	3%	0.3	8%	179	4%	0.1	5%	95	5%
	T	0.5	26%	562	5%	0.3	8%	172	3%	0.1	5%	43	4%
	TTV	0.4	34%	19	3%	0.2	11%	396	13%	0.2	7%	413	16%
	TTVV	0.4	34%	109	3%	0.2	9%	381	4%	0.1	5%	536	2%
	TVV	0.6	30%	4	6%	0.2	11%	305	4%	0.1	6%	428	8%
	V	0.3	30%	229	1%	0.2	7%	179	2%	0.0	5%	148	5%
HIAC	R	0.7	17%	108	2%	0.6	19%	357	3%	0.5	9%	481	4%
	C	0.7	17%	108	2%	0.6	17%	289	3%	0.5	9%	490	6%
	T	0.7	17%	81	1%	0.6	17%	314	2%	0.6	9%	491	3%
	TTV	0.7	14%	1176	31%	1.1	14%	435	7%	0.6	11%	313	6%
	TTVV	0.8	13%	189	3%	1.0	11%	220	3%	0.8	9%	157	4%
	TVV	0.8	13%	1347	1%	1.0	13%	424	4%	0.8	10%	268	6%
	V	0.7	12%	55	2%	1.0	12%	417	2%	0.5	10%	498	3%
Syringe 670 nm	R	0.5	26%	140	1%	0.0	7%	27	0%	0.0	4%	30	2%
	C	0.4	27%	181	3%	0.1	7%	84	2%	0.0	4%	65	4%
	T	0.4	27%	181	2%	0.1	7%	82	2%	0.0	4%	51	1%
	TTV	0.5	32%	141	4%	0.0	9%	88	3%	0.1	5%	72	4%
	TTVV	0.4	32%	197	8%	0.1	8%	153	9%	0.2	5%	156	12%
	TVV	0.3	32%	228	8%	0.1	8%	186	8%	0.2	5%	207	8%
	V	0.3	26%	132	7%	0.1	8%	112	8%	0.1	5%	99	6%
Syringe 780 nm	R	0.6	19%	27	1%	0.2	7%	5	1%	0.0	3%	46	1%
	C	0.5	19%	58	1%	0.2	6%	56	2%	0.0	2%	51	3%
	T	0.6	19%	96	1%	0.2	7%	91	1%	0.0	3%	86	1%
	TTV	0.6	24%	73	3%	0.3	11%	32	3%	0.1	7%	84	2%
	TTVV	0.7	21%	65	5%	0.0	10%	51	5%	0.1	6%	112	7%
	TVV	0.7	22%	23	2%	0.0	12%	54	2%	0.1	7%	152	2%
	V	0.6	18%	22	3%	0.3	11%	7	6%	0.0	7%	20	8%

Table 11: performance overview of sample matrix influence for borosilicate glass sphere standards suspended in water as reference media (R), colored matrix (C), opalescent matrix (T), 35 FTU at 11 mPa*s (TTV), 30 FTU at 20 mPa*s (TTVV), 16 FTU at 20 mPa*s (TVV) and clear at 11 mPa*s (V). For the individual samples following key parameters are shown: counting accuracy: the difference between the observed particle size (n=10000) and the suppliers certified size in µm ($\Delta M_{ø}$); sizing precision: the sensor resolution according to EP/USP in % ($CV_{ø}$); counting accuracy: the difference between the calculated value and the observed mean particle counts (n=4) in particles per ml ($\Delta M_{\#}$); counting precision the standard deviation devided by the mean particle counts n=4 individual measurements in % (CV#). The individual columns are colored in gradient from low to high performance (BAD NEUTRAL GOOD)

		Borosilicate glass spheres							
		2µm				8µm			
		$\Delta M_{ø}$	$CV_{ø}$	$\Delta M_{\#}$	$CV_{\#}$	$\Delta M_{ø}$	$CV_{ø}$	$\Delta M_{\#}$	$CV_{\#}$
FloCam 10x	R	0.1	33%	28	4%	1.0	18%	336	6%
	C	0.1	33%	7	7%	0.9	17%	283	9%
	T	0.1	31%	60	5%	1.0	18%	176	8%
	TTV	0.2	48%	1949	3%	1.7	15%	1360	2%
	TTVV	0.2	42%	310	58%	1.5	17%	169	46%
	TVV	0.1	38%	1170	29%	1.3	20%	143	27%
	V	0.2	36%	264	5%	0.7	16%	908	6%
MFI 5x	R	0.3	14%	9	4%	0.3	7%	8	7%
	C	0.3	14%	168	10%	0.5	7%	350	29%
	T	0.3	15%	12	30%	0.4	6%	98	62%
	TTV	0.2	29%	441	17%	0.3	16%	477	26%
	TTVV	0.3	26%	184	19%	0.1	10%	125	24%
	TVV	0.3	29%	422	54%	0.2	14%	438	71%
	V	0.0	36%	71	27%	0.5	11%	11	52%
HIAC	R	0.4	32%	312	4%	0.6	10%	366	2%
	C	0.4	31%	313	7%	0.7	8%	400	5%
	T	0.4	31%	272	5%	0.7	7%	377	4%
	TTV	0.6	24%	3589	4%	0.7	15%	716	12%
	TTVV	0.5	29%	191	58%	0.8	11%	103	73%
	TVV	0.5	31%	1699	10%	1.0	15%	1206	12%
	V	0.4	34%	432	32%	1.0	11%	502	42%
Syringe 670 nm	R	0.0	32%	155	3%	0.0	4%	191	1%
	C	0.1	25%	50	2%	0.2	0%	185	2%
	T	0.1	25%	51	1%	0.2	0%	160	1%
	TTV	0.2	35%	8	53%	0.8	16%	619	61%
	TTVV	0.2	35%	355	69%	0.4	13%	26	87%
	TVV	0.2	38%	189	50%	0.6	14%	276	60%
	V	0.1	37%	310	8%	0.2	8%	101	8%
Syringe 780 nm	R	0.0	34%	301	5%	0.0	9%	151	3%
	C	0.3	19%	152	3%	0.2	5%	141	3%
	T	0.3	18%	253	30%	0.2	6%	51	40%
	TTV	0.3	32%	197	28%	0.1	16%	269	33%
	TTVV	0.3	28%	197	3%	0.1	14%	305	4%
	TVV	0.4	30%	119	16%	0.1	12%	464	18%
	V	0.3	28%	305	17%	0.4	11%	25	20%

Next Steps / Outlook

Several analytical aspects related to the testing and measuring of SbVP, for example by MDI and LO, warrant further investigation.

FlowCam and MFI provide a great opportunity for particle characterization, while their ability for particle counting remains to be further validated, especially in a QC environment. In this context, image quality is a key parameter for morphological analysis of particles. Improving image contrast for translucent particles would be beneficial, e.g. by using phase contrast microscopy or darkfield microscopy implemented into the MDI. Though the limit of resolution due to diffraction is already been addressed, e.g. in photo activated localization microscopy, it will take some time for this technology to become applicable in flow microscopy.[33,34]

Besides the improvement of image quality and MDI technology, some work should be investigated in terms of defining morphological parameters, including their relevance and application to therapeutic protein solutions. As demonstrated in this thesis, different particle types can only be resolved to a certain extent, even when considering recent improvements by combining more than one parameter.[35] A so called "f-factor" was introduced recently, providing better capability to differentiate between silicone oil droplets and protein particles.[35] With regards to counting and sizing protein-based particles in a QC environment, the need for the development of a stable reference standard, that resembles key properties of protein particles, has been suggested to help fully validate MDI instruments for particle counting. Various groups have started to characterize the different types of protein particles according to their origin and morphology.[36-38] However, to date, polystyrene bead standards still remain the gold standard for instrument standardization, calibration, method development, verification and validation, especially for use in a QC environment.

References

1. Ph.Eur. 2011. 2.9.19. Particulate contamination: sub-visible particles. 7 ed.: European Directorate for the Quality of Medicine (EDQM).

2. USP. 2011. General Chapter <1788> Particulare Matter Determination in Parenteral and Opthalmic Products. USP34-NF29 ed., Rockville, MD: United States Pharmacopeial Convention.

3. USP. 2011. General Chapter <788> Particulare Matter Determination in Injections. USP34-NF29 ed., Rockville, MD: United States Pharmacopeial Convention.

4. Sharma DK, Oma P, King D 2009. Applying Intelligent Flow Microscopy to Biotechnology. BioProcess International 7(6):62-67.

5. Sharma DK, King D, Oma P, Merchant C 2010. Micro-flow imaging: flow microscopy applied to sub-visible particulate analysis in protein formulations. The AAPS journal 12(3):455-464.

6. Huang CT, Sharma D, Oma P, Krishnamurthy R 2009. Quantitation of protein particles in parenteral solutions using micro-flow imaging. Journal of pharmaceutical sciences 98(9):3058-3071.

7. Sharma DK, Oma P, Pollo MJ, Sukumar M 2010. Quantification and characterization of subvisible proteinaceous particles in opalescent mAb formulations using micro-flow imaging. Journal of pharmaceutical sciences 99(6):2628-2642.

8. Singh SK, Afonina N, Awwad M, Bechtold-Peters K, Blue JT, Chou D, Cromwell M, Krause HJ, Mahler HC, Meyer BK, Narhi L, Nesta DP, Spitznagel T 2010. An industry perspective on the monitoring of subvisible particles as a quality attribute for protein therapeutics. Journal of pharmaceutical sciences 99(8):3302-3321.

9. Carpenter JF, Randolph TW, Jiskoot W, Crommelin DJ, Middaugh CR, Winter G, Fan YX, Kirshner S, Verthelyi D, Kozlowski S, Clouse KA, Swann PG, Rosenberg A, Cherney B 2009. Overlooking subvisible particles in therapeutic protein products: gaps that may compromise product quality. Journal of pharmaceutical sciences 98(4):1201-1205.

10. Ripple DC, Wayment JR, Carrier MJ 2011. Standards for the Optical Detection of Protein Particles. A Pharm Review:90-96.

11. Narhi LO, Jiang Y, Cao S, Benedek K, Shnek D 2009. A critical review of analytical methods for subvisible and visible particles. Current pharmaceutical biotechnology 10(4):373-381.

12. Oma P, Deepak Sharma, King D 2010. Flow Microscopy: Dynamic Image Analysis for Particle Counting. Pharmacopeial Forum 36(1):311-320.

13. Liu L, Ammar DA, Ross L, Mandava N, Kahook M, Carpenter J 2011. Silicone Oil Microdroplets and Protein Aggregates in Repackaged Bevacizumab and Ranibizumab: Effects of Long-term Storage and Product Mishandling. Investigative ophthalmology & visual science 52(2):1023-1034.

14. Wuchner K, Buchler J, Spycher R, Dalmonte P, Volkin DB 2010. Development of a microflow digital imaging assay to characterize protein particulates during storage of a high concentration IgG1 monoclonal antibody formulation. Journal of pharmaceutical sciences 99(8):3343-3361.

15. Demule B, Messick S, Shire SJ, Liu J 2010. Characterization of particles in protein solutions: reaching the limits of current technologies. The AAPS journal 12(4):708-715.

16. Chrai S, Clayton R, Mestrandrea L, Myers T, Raskin R, Sokol M, Willis C 1987. Limitations in the use of HIAC for product particle counting. J Parenter Sci Technol 41(6):209-214.

17. Kanai S, Liu J, Patapoff TW, Shire SJ 2008. Reversible self-association of a concentrated monoclonal antibody solution mediated by Fab-Fab interaction that impacts solution viscosity. Journal of pharmaceutical sciences 97(10):4219-4227.

18. Liu J, Nguyen MD, Andya JD, Shire SJ 2005. Reversible self-association increases the viscosity of a concentrated monoclonal antibody in aqueous solution. Journal of pharmaceutical sciences 94(9):1928-1940.

19. Li B, Flores J, Corvari V 2007. A simple method for the detection of insoluble aggregates in protein formulations. Journal of pharmaceutical sciences 96(7):1840-1843.

20. Kishore RS, Kiese S, Fischer S, Pappenberger A, Grauschopf U, Mahler HC 2011. The Degradation of Polysorbates 20 and 80 and its Potential Impact on the Stability of Biotherapeutics. Pharmaceutical research 28(5):1194-1210.

21. Kishore RS, Pappenberger A, Dauphin IB, Ross A, Buergi B, Staempfli A, Mahler HC 2010. Degradation of polysorbates 20 and 80: Studies on thermal autoxidation and hydrolysis. Journal of pharmaceutical sciences 100(2):721-731.

22. Ph.Eur. 2011. 2.2.2 Degree of coloration of liquids. 7 ed.: European Directorate for the Quality of Medicine (EDQM).

23. Ph.Eur. 2011. 2.2.1 Clarity and degree of opalescence of liquids. 7 ed.: European Directorate for the Quality of Medicine (EDQM).

24. Kiese S, Papppenberger A, Friess W, Mahler HC 2008. Shaken, not stirred: mechanical stress testing of an IgG1 antibody. Journal of pharmaceutical sciences 97(10):4347-4366.

25. Cao S, Jiao N, Jiang Y, Mire-Sluis A, Narhi LO 2009. Sub-visible particle quantitation in protein therapeutics. Pharmeuropa bio & scientific notes 2009(1):73-79.

26. Barber TA, Lannis MD, Williams JG, Ryan JF 1990. Application of improved standardization methods and instrumentation in the USP particulate test for SVI. J Parenter Sci Technol 44(4):185-203.

27. USP. 2011. General Chapter <1061> Color - instrumental measurement. USP34-NF29 ed., Rockville, MD: United States Pharmacopeial Convention.

28. Hopkins KD, Weeks DL 1990. Tests for Normality and Measures of Skewness and Kurtosis: Their Place in Research Reporting. Educational and Psychological Measurement 50(4):717-729.

29. DeCarlo 1997. On the Meaning and Use of Kurtosis. Psychological Methods 2(3):292-307.

30. Oma P, Sharma D, King D 2010. Flow Microscopy: Dynamic Image Analysis for Particle Counting. Pharmacopeial Forum 36(1):311-320.

31. Hartung J. 2009. Statistik: Lehr- und Handbuch der angewandten Statistik 14 ed.: Oldenbourg Wissenschaftsverlag.

32. Hendricks WA, Robey KW 1936. The Sampling Distribution of the Coefficient of Variation. Annals of Mathematical Statistics 7(3):129-132.

33. Rust MJ, Bates M, Zhuang X 2006. Sub-diffraction-limit imaging by stochastic optical reconstruction microscopy (STORM). Nature Methods 3(10): 793 - 796.

34. Hess ST, Girirajan TPK, Mason MD 2006. Ultra-High Resolution Imaging by Fluorescence Photoactivation Localization Microscopy. Biophysical journal 91(11):4258-4272.

35. Strehl R, Rombach-Riegraf V, Diez M, Egodage K, Bluemel M, Jeschke M, Koulov AV 2011. Discrimination Between Silicone Oil Droplets and Protein Aggregates in Biopharmaceuticals: A Novel Multiparametric Image Filter for Sub-visible Particles in Microflow Imaging Analysis. Pharmaceutical research 2011 ePub.

36. Narhi LO, Schmit J, Bechtold-Peters K, Sharma D 2011. Classification of protein aggregates. Journal of pharmaceutical sciences 2011 ePub.

37. Luo Q, Joubert MK, Stevenson R, Ketchem RR, Narhi LO, Wypych J 2011. Chemical modifications in therapeutic protein aggregates generated under different stress conditions. The Journal of biological chemistry 286(28):25134-25144.

38. Joubert MK, Luo Q, Nashed-Samuel Y, Wypych J, Narhi LO 2011. Classification and characterization of therapeutic antibody aggregates. The Journal of biological chemistry 286(28):25118-25133.